Chapter 1

Binding Energy and the SEMF

> *"Attempting to understand this curve of binding energy leads us to the semiempirical mass formula."*
>
> K. S. Krane

Lectures 1–3 fixed the nuclear *size*: charge densities, saturation, and finite-size shifts. This lecture turns to nuclear *energy*: how tightly nucleons stick together, and how that energy varies with A and Z. Binding energy is the mass defect of the nucleus written as an energy. The semi-empirical mass formula (SEMF) is a five-parameter model of $B(A, Z)$ that organises the chart of nuclides and the B/A curve [6, 1, 13, 14, 2].

Key idea

Binding energy is the mass defect of the nucleus written as an energy. The SEMF is a five-parameter model of $B(A, Z)$ that organises the chart of nuclides and the B/A curve.

1.1 Why not every (Z, N) combination is a nucleus?

Not every combination of protons and neutrons forms a stable (or even bound) nucleus. Ten free protons do not assemble into a long-lived $Z = 10$, $N = 0$ system; ten free neutrons do not form a stable droplet either. Here it is important to separate *existence* from *stability*. A nuclide may be bound against immediate nucleon emission yet radioactive against beta decay, alpha decay, or fission. The chart of nuclides is therefore a narrow ribbon in the (N, Z) plane: outside that ribbon, systems either beta decay toward lower-mass isobars or, beyond the drip lines, cannot bind the last nucleon at all [14, 6, 1].

Stability is a competition among three physical agents, each with a different range and different A, Z dependence:

- **short-range strong attraction** among nearest neighbours, which wants as many nucleons packed at saturation density as possible and scales roughly with the nuclear volume;
- **long-range Coulomb repulsion** among protons, which wants fewer protons at fixed A and grows roughly as Z^2/R;
- **quantum statistics and pairing**: the Pauli principle gives separate proton and neutron

Fermi seas and penalises a large imbalance $N - Z$, while an additional attractive pairing correlation favours even proton and neutron numbers.

No single force wins everywhere. Light nuclei hug $N = Z$ because asymmetry energy dominates Coulomb. Heavy nuclei drift to $N > Z$ because Coulomb grows faster with Z than the asymmetry cost of a moderate neutron excess. Far from the ribbon, the last neutron or proton is unbound: those loci are the neutron and proton drip lines predicted semi-quantitatively by the SEMF and mapped experimentally with radioactive beams [14, 1].

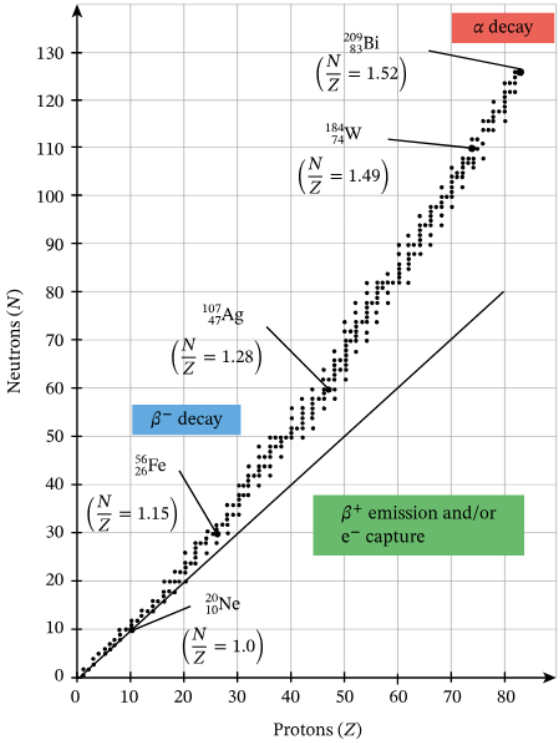

Figure 1.1: Chart of nuclides in the N–Z plane (valley of stability). Light nuclei prefer $N \approx Z$; heavy nuclei need $N > Z$. Nuclei off the valley return by $\beta^{\pm}$ (or electron capture) and, for heavy species, also by α emission; the drip lines mark where nucleon separation energies vanish.

Figure 1.1 is the experimental map we must eventually explain. Nuclei with a measured mass m are lighter than the free nucleons from which they are assembled. That mass defect is the **binding energy** B. A systematic study of $B(A, Z)$, and especially of the average B/A, leads to a few-parameter model of nuclear binding: the liquid-drop picture and the semi-empirical mass formula (SEMF) [6, 1, 2, 14]. The SEMF will not predict shell closures or spectroscopic details, but it organises why the valley exists, why $B/A \sim 8\,\mathrm{MeV}$, and why fusion and fission both release energy.

1.2 Total energy of a nucleus: derivation from rest masses

The preceding survey explains why energy comparison is the natural next step: a proposed (Z, N) combination can persist only when no allowed route leads to a lower-energy set of products. Before constructing the SEMF, we must therefore distinguish three energies that are often compressed into a single formula:

1. the rest energy of Z free protons and N free neutrons;

2. the smaller rest energy of the bound nucleus;

3. the rest energy of the neutral atom whose mass is actually tabulated.

The derivation below keeps all three ledgers explicit.

1.2.1 Separated nucleons versus a bound nucleus

Imagine first that every constituent is at rest and separated by arbitrarily large distances, so that their mutual interactions vanish. Taking this separated configuration as the reference threshold gives

$$E_{\text{free}} = Zm_pc^2 + Nm_nc^2. \tag{1.1}$$

The rest masses in Equation (1.1) already include each nucleon's internal quark and gluon energy. What is absent is the energy associated with their relative motion and their mutual nuclear and Coulomb interactions. For a nonrelativistic nuclear Hamiltonian this bookkeeping may be displayed schematically as

$$H = Zm_pc^2 + Nm_nc^2 + T_{\text{rel}} + V_{\text{strong}} + V_{\text{C}} + \cdots . \tag{1.2}$$

Here $T_{\text{rel}} > 0$, whereas the expectation value of the attractive part of V_{strong} is negative. Coulomb repulsion raises the energy. A bound state exists only when all contributions after the rest masses combine to a negative eigenvalue.

When the free nucleons assemble into a nucleus, energy is carried away by photons, emitted particles, or recoil. If the final nucleus is left in its ground state, the maximum released energy is the binding energy $B(A, Z)$. Conversely, precisely this energy must be supplied to reach the separated-nucleon threshold. Energy conservation may therefore be written

$$E_{\text{nuc}} + B = E_{\text{free}}. \tag{1.3}$$

Since the nucleus at rest has $E_{\text{nuc}} = M_{\text{nuc}}(A, Z)c^2$, it follows step by step that

$$M_{\text{nuc}}(A, Z)c^2 = Zm_pc^2 + Nm_nc^2 - B(A, Z), \tag{1.4}$$

$$B(A, Z) = \Big[Zm_p + Nm_n - M_{\text{nuc}}(A, Z)\Big]c^2. \tag{1.5}$$

Thus the *total internal-energy shift* of a bound nucleus is negative when the zero is chosen at separated nucleons:

$$E_{\text{internal}} = E_{\text{nuc}} - E_{\text{free}} = \langle T_{\text{rel}} + V_{\text{strong}} + V_{\text{C}} + \cdots \rangle = -B. \tag{1.6}$$

The binding energy B is quoted as a positive number, while the energy shift of the bound state is $-B$. These two sign conventions describe the same physics. It would be incorrect to identify $-B$ with the potential energy alone: confined nucleons have positive kinetic energy, so the attractive potential must be more negative than $-B$.

Why the minimum of total energy determines stability

At fixed $A = N + Z$, beta processes convert a neutron into a proton or a proton into a neutron. They therefore move between neighbouring isobars. The comparison must include every particle in the initial and final states. Neutral atomic masses do this bookkeeping conveniently:

$$Q_{\beta^-} = \left[M_{\rm at}(A,Z) - M_{\rm at}(A,Z+1)\right]c^2, \tag{1.7}$$

$$Q_{\beta^+} = \left[M_{\rm at}(A,Z) - M_{\rm at}(A,Z-1) - 2m_e\right]c^2, \tag{1.8}$$

$$Q_{\rm EC} \simeq \left[M_{\rm at}(A,Z) - M_{\rm at}(A,Z-1)\right]c^2, \tag{1.9}$$

apart from small electron-binding and recoil corrections. A channel is energetically open only when its Q value is positive. Thus the stable member of an isobaric chain lies at an allowed minimum of the *atomic* mass, subject also to selection rules. Lecture 5 develops this idea into the mass parabola $M(A,Z)$.

1.2.2 Binding is necessary but not sufficient for stability

Equation (1.5) answers one specific question: is the nucleus below the threshold of Z free protons plus N free neutrons? If $B > 0$, complete breakup into free nucleons costs energy. That does *not* prove that the nuclide is stable. A different partition, such as an α particle plus a daughter nucleus, may have a still lower total energy; a neighbouring isobar may be accessible through beta decay; and a heavy nucleus may lower its energy by fission. For any proposed decay

$$P \longrightarrow 1 + 2 + \cdots ,$$

the decisive quantity is

$$Q = \left(M_P - \sum_f M_f \right) c^2. \tag{1.10}$$

Positive Q means that energy conservation permits the decay, with Q becoming kinetic energy or radiation. Whether the decay is rapid then depends on the interaction involved, angular-momentum and parity selection rules, and possible barriers. Consequently:

- **bound** means below a specified breakup threshold;
- **energetically stable** means no allowed final state has lower total energy;
- **long-lived** may instead mean that a lower-energy channel exists but is strongly hindered, as in alpha decay or spontaneous fission.

1.2.3 Why experiments use atomic masses

Bare nuclear masses are less convenient experimentally than neutral atomic masses. Add the rest energy of Z free electrons to both sides of Equation (1.4):

$$M_{\rm nuc}c^2 + Zm_ec^2 = Z(m_p + m_e)c^2 + Nm_nc^2 - B. \tag{1.11}$$

Neither side is yet an atomic mass, because binding the electrons also lowers the energy. Let $B_e(Z, A) > 0$ denote the total electronic binding energy of the neutral atom. Its mass satisfies

$$M_{\text{at}}(A, Z)c^2 = M_{\text{nuc}}(A, Z)c^2 + Zm_e c^2 - B_e(Z, A). \tag{1.12}$$

For a ground-state hydrogen atom,

$$m(^1\text{H})c^2 = (m_p + m_e)c^2 - B_{\text{H}}, \qquad B_{\text{H}} = 13.6\,\text{eV}, \tag{1.13}$$

and hence

$$(m_p + m_e)c^2 = m(^1\text{H})c^2 + B_{\text{H}}. \tag{1.14}$$

Substitute Equations (1.12) and (1.13) into Equation (1.11). The exact atomic-mass relation is

$$\begin{aligned} M_{\text{at}}(A, Z)c^2 = {} & Zm(^1\text{H})c^2 + Nm_n c^2 - B(A, Z) \\ & + ZB_{\text{H}} - B_e(Z, A). \end{aligned} \tag{1.15}$$

Solving this equation for the nuclear binding energy gives

$$\begin{aligned} B(A, Z) = {} & \Big[Zm(^1\text{H}) + Nm_n - M_{\text{at}}(A, Z)\Big]c^2 \\ & + ZB_{\text{H}} - B_e(Z, A). \end{aligned} \tag{1.16}$$

This is the complete derivation of the nuclear binding energy from tabulated atomic masses. Notice that electron rest masses have not merely been discarded: they cancel because each proton on the separated side is paired with one electron to form a hydrogen atom. Only the much smaller difference between electronic *binding* energies remains.

1.2.4 Controlled approximation used in nuclear physics

The electronic correction in the second line of Equation (1.16) is small on a nuclear scale. The hierarchy is

$$\begin{aligned} & B_{\text{H}} = 13.6\,\text{eV}, \qquad B_e(Z, A) \sim \text{keV–1 MeV} \quad \text{(medium to very heavy atoms)}, \\ & B_{\text{nuc}} \sim \text{MeV–GeV}. \end{aligned} \tag{1.17}$$

Even a binding energy of tens of MeV is millions of times larger than the hydrogen ionisation energy. In heavy nuclei the nuclear binding is typically hundreds of MeV to more than a GeV, whereas total electronic binding remains at most of order MeV. Therefore, unless high-precision mass differences are required, one neglects $ZB_{\text{H}} - B_e$ and obtains

$$\boxed{B(A, Z) \simeq \Big[Zm(^1\text{H}) + Nm_n - M_{\text{at}}(A, Z)\Big]c^2.} \tag{1.18}$$

The approximation does not mean that electron binding is zero. It means that the difference of electronic binding terms is much smaller than the nuclear binding being extracted. Precision mass evaluations restore that correction when necessary.

1.3 Practical mass quantities

Section 1.2 has already established the physical meaning of B, the exact conversion between nuclear and atomic masses, and the approximation in Equation (1.18). We now use that result rather than derive it again. Throughout the remainder of this lecture, $M_{\mathrm{at}}(A, Z)$ denotes a neutral atomic mass, and $N = A - Z$.

1.3.1 Mass units and a numerical example

Atomic masses are normally quoted in unified atomic mass units. The mass–energy conversion is

$$1\,\mathrm{u}\,c^2 = 931.494\,\mathrm{MeV} \approx 931.5\,\mathrm{MeV}. \tag{1.19}$$

Thus a seemingly small mass defect of 10^{-2} u corresponds to nearly 10 MeV, which is a natural nuclear-energy scale. When the SEMF is converted into an atomic-mass formula in this lecture, we use

$$M_{\mathrm{at}}(A, Z) \simeq Z m(^1\mathrm{H}) + N m_n - \frac{B(A, Z)}{c^2}.$$

This is an atomic-mass convention for applying the SEMF, with the electronic correction derived in Equation (1.16) neglected; the binding-energy formula itself is a model of the nucleus and does not depend on that bookkeeping choice [4].

Mass defect and B

For the α particle, the relevant mass defect is approximately $\Delta m = 0.0304\,\mathrm{u}$. Therefore

$$B = \Delta m\, c^2 \approx (0.0304\,\mathrm{u})(931.494\,\mathrm{MeV/u}) \approx 28.3\,\mathrm{MeV}.$$

Dividing by four gives $B/A \approx 7.07\,\mathrm{MeV}$, exceptionally large for so light a system. This strong binding helps explain the prominence of alpha clustering and alpha-decay products (see Problem 4.1) [6, 1, 2].

1.3.2 Mass excess

Many tables quote the **mass excess** (also called mass defect in some older tables)

$$\Delta(A, Z) \equiv [M_{\mathrm{at}}(A, Z) - A\,\mathrm{u}]c^2 \tag{1.20}$$

in MeV rather than the atomic mass itself [1, 6]. Because $A \cdot \mathrm{u}$ is an integer number of mass units, differences of mass excesses are differences of mass energies. Binding energies and Q values can be written entirely in terms of Δ's. For example, once $\Delta(^A X)$, $\Delta(^1\mathrm{H})$, and $\Delta(n)$ are known, (1.18) becomes an arithmetic combination of tabulated MeV values. We keep the mass form (1.18) in the main text for transparency.

1.3.3 Separation energies

Just as atomic ionisation energies probe the outermost electron, nucleon separation energies probe the outermost nucleon. The neutron and proton separation energies are

$$S_n(A,Z) = B(A,Z) - B(A-1,Z) = \big[M_{\rm at}(A-1,Z) + m_n - M_{\rm at}(A,Z)\big]c^2, \tag{1.21}$$

$$S_p(A,Z) = B(A,Z) - B(A-1,Z-1) = \big[M_{\rm at}(A-1,Z-1) + m(^1\mathrm{H}) - M_{\rm at}(A,Z)\big]c^2. \tag{1.22}$$

The atomic-mass bookkeeping is deliberate: $m(^1\mathrm{H})$ appears in S_p rather than m_p, so that electron masses cancel exactly as they do in B [6]. Odd–even staggering in S_n is direct evidence for pairing (pairing section below). Shell closures appear as jumps in separation energies (shell model, later). In the one-nucleon criterion, the neutron and proton drip lines occur when S_n or S_p reaches zero: adding one more nucleon no longer increases B, so the system is unbound against that emission channel. Pairing can make two-nucleon separation energies relevant as well [14, 1].

1.4 The curve of B/A: what must be explained

Because B grows roughly linearly with A, it is standard to plot the average binding energy per nucleon,

$$\frac{B}{A} = (\text{total binding energy})/(\text{number of nucleons}), \tag{1.23}$$

against A. This curve is the central experimental object of nuclear structure at the bulk level: it compresses thousands of measured masses into one smooth trend plus small ripples. Attempting to understand it leads to the SEMF, in which a few general parameters characterise how B varies with A and Z [6]. If B were strictly proportional to A, the plot would be a horizontal line at about 8 MeV; every deviation from that line is a clue about the nuclear force, nuclear geometry, or quantum statistics [1, 13].

1.4.1 Features of the experimental curve

Several remarkable features stand out on the experimental B/A curve [6, 1, 14, 13, 2, 5, 4]:

1. **Nearly constant B/A.** Except for the very lightest nuclei,

$$7.7\,\mathrm{MeV} \lesssim B/A \lesssim 8.8\,\mathrm{MeV}$$

   for stable species with $12 \lesssim A \lesssim 225$, or more loosely "between 7 and 9 MeV per nucleon." That is why one often says "about 8 MeV per nucleon." To within about 10%, most nuclei share this scale [6].

2. **Broad maximum in the iron–nickel region** ($A \sim 56$–62): the most tightly bound nuclei *per nucleon*. The smooth liquid-drop curve peaks near ^{56}Fe; precise atomic-mass data give the highest B/A at ^{62}Ni, with ^{58}Fe and ^{56}Fe only slightly lower [4, 14]. For energy release in stars and reactors, "iron peak" is the right mental picture even though the exact maximum nuclide is nickel-62.

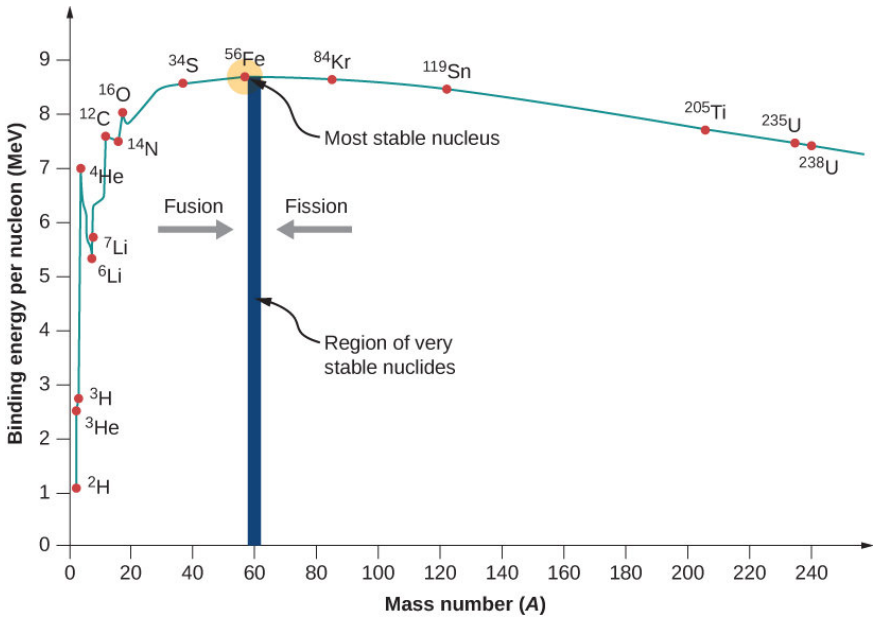

Figure 1.2: Binding energy per nucleon versus mass number. The curve is roughly flat near 8 MeV, peaks in the iron–nickel region, and falls slowly for heavy nuclei. Light $A = 4n$ species (^{4}He, ^{12}C, ^{16}O) sit above the smooth trend. Modern mass tables place the absolute maximum of B/A at ^{62}Ni, with ^{58}Fe and ^{56}Fe very close; the iron peak is the practical reference for fusion and stellar burning [6, 4].

3. **Rise at low A.** Light nuclei have a larger fraction of surface nucleons, so B/A climbs as A increases and the surface/volume ratio falls.

4. **Slow decline for heavy A.** Coulomb repulsion among many protons gradually wins; B/A falls toward uranium and beyond.

5. **Two ways to release energy.** Climbing the curve from below ($A \lesssim 56$) is fusion; climbing from above ($A \gtrsim 56$) is fission. Both increase B/A and therefore release energy. The light side of the curve is the domain of stellar nuclear burning; the heavy side is the domain of fission and α decay [14, 5, 13].

6. **Fine structure.** Odd–even staggering (pairing) and extra binding of light $A = 4n$ nuclei (α clustering: ^{4}He, ^{12}C, ^{16}O) sit on top of the smooth trend. Notably, ^{8}Be lies slightly *below* two α particles and therefore decays into them [2]. The SEMF captures the smooth part, not every shell or cluster peak.

1.4.2 Which SEMF term explains which feature?

The rest of this lecture builds the SEMF term by term. It helps to know in advance how each piece of the curve will be accounted for:

Feature on B/A	**SEMF term(s) responsible**
Nearly flat $\sim 8\,\text{MeV}$ for $12 \lesssim A \lesssim 225$	Volume $+a_V A$: short-range saturation gives $B \propto A$ and $B/A \sim a_V$ before corrections.
Rise from very light A	Surface $-a_S A^{2/3}$: at small A the surface/volume ratio is large, so $\lvert B_S\rvert/A \propto A^{-1/3}$ is a big penalty that falls as A grows.
Broad maximum near iron–nickel	Competition of surface (favours larger A) and Coulomb (favours smaller Z, hence limits growth of A for a given valley N/Z).
Slow decline past the peak	Coulomb $-a_C Z(Z-1)/A^{1/3}$: $\lvert B_C\rvert/A$ grows for heavy systems with many protons.
Valley of stability ($N \approx Z$ at light A, $N > Z$ at heavy A)	Coulomb plus asymmetry $-a_{\text{a}}(N-Z)^2/A$: Coulomb alone would push $Z \to 0$; asymmetry restores $N \sim Z$ when Coulomb is weak and permits controlled neutron excess when it is strong.
Odd–even ripples on B/A	Pairing δ: even–even nuclei gain a few hundred keV per nucleon; odd–odd lose a similar amount.
Spikes at ^{4}He, ^{12}C, ^{16}O	Beyond the SEMF: α clustering and shell structure (later chapters).

The liquid-drop model explains the *smooth* envelope. Shell and cluster effects are superimposed as corrections of order 1 MeV or less per nucleon on top of the $\sim 8\,\text{MeV}$ bulk scale [6, 1].

Key idea

First clue about the force. If every nucleon attracted every other nucleon with a long-range force, we would expect $B \propto A(A-1) \sim A^2$ and $B/A \propto A$. Experiment gives $B \propto A$ and $B/A \sim$ const. Therefore each nucleon interacts only with its nearest neighbours. Combined with constant density (Lecture 2), that is the signature of a short-range force of range comparable to the internucleon spacing [6, 1].

1.4.3 Why $B \propto A$ is surprising (and important)

A long-range force among A particles produces $\binom{A}{2} \sim A^2/2$ pairs. Gravity and Coulomb are of that type (every mass attracts every mass; every charge feels every charge). The strong residual force is not: saturated nuclear matter has fixed density and fixed coordination number, so the total binding scales with the number of particles, not the number of pairs [6, 1, 13].

From electron scattering we already know that the nuclear density is roughly constant, so each nucleon has about the same number of neighbours and contributes roughly the same amount to the binding energy [6]. The same linear behaviour is consistent with the short-range conclusions drawn from nucleon-density systematics in the previous chapters [1].

That observation is the starting point of the liquid-drop model.

1.5 The liquid-drop idea

The liquid-drop model is a *semi-empirical* model of $B(A, Z)$ [1, 6, 12, 14, 2]:

- **semi:** the algebraic form of each term is motivated by physics (geometry, electrostatics, quantum statistics);
- **empirical:** the numerical coefficients are fixed by fitting measured masses.

The idea goes back to Bohr (1935): the short range of nuclear forces, together with additivity of volumes and of binding energies, invites a liquid-drop description [14]. The same empirical fact drives the analogy from another direction: the nearly homogeneous mass density inside the nucleus suggests comparing the nucleus with a liquid drop in which the main part of the interaction is only between nearest neighbours [2]. In practice the model describes how the nuclear binding energy depends on neutron and proton number, and it is an effective way to organise the relative stability of nuclides [1].

Why a "drop"? Nuclei and classical liquid drops share

1. many constituents;
2. nearly constant interior density (incompressibility at leading order; volume $\propto A$);
3. a well-defined surface with surface tension;
4. short-range cohesion among neighbours (like molecules in a water droplet, or van der Waals cohesion in a classical liquid).

One must *not* identify the nuclear force with van der Waals forces; only the geometry of a saturating short-range interaction is borrowed [1]. The analogy is useful for energetics, not for microscopic dynamics.

The first three SEMF terms (volume, surface, Coulomb) would appear in the energy of any charged liquid droplet. The last two (asymmetry, pairing) are quantum and have no pure classical analogue: they encode Pauli filling of two fermion species and the tendency of like nucleons to form $J = 0$ pairs [6, 14, 13]. In that sense the SEMF is a first attempt to apply nuclear models to systematic behaviour: liquid-drop physics for the gross collective features, and shell/quantum ingredients for the last two terms [6].

Throughout we assume a spherical nucleus to leading order (a good approximation for most ground states near stability) and a nuclear volume directly related to A [1, 4]. Deformations and shell corrections refine that picture later; they are not needed to understand the smooth B/A curve.

1.5.1 Historical development: Gamow, Weizsäcker, Bethe

The picture of the nucleus as a charged liquid drop was developed in the early 1930s by **George Gamow**. The quantitative mass formula was written down by **Carl Friedrich von Weizsäcker** in 1935 ("Zur Theorie der Kernmassen") as the **semi-empirical mass formula**, and refined the same year by **Hans Bethe** and collaborators. The formula is therefore often called the **Bethe–Weizsäcker** (or SEMF) formula [12, 6, 1, 14, 4]. The numerical coefficients are chosen to

approximate observed ground-state binding energies; other than a_C (which is largely calculable from electrostatics), they are fixed empirically [14, 1].

Historical note: George Gamow (1904–1968)

George Gamow (born Georgiy Antonovich Gamov in Odessa) was a Soviet-American theoretical physicist and cosmologist. In the late 1920s he explained α decay as quantum tunnelling through the Coulomb barrier. In the early 1930s he developed the *liquid-drop* picture of the nucleus: nucleons packed at roughly constant density, held by a short-range attraction analogous to the cohesion of a liquid, with a surface and a Coulomb self-energy of the proton charge. That geometric intuition is the starting point of the SEMF volume, surface, and Coulomb terms. After leaving the Soviet Union he worked in the United States (George Washington University, later Colorado), co-authored the Alpher–Bethe–Gamow paper on Big Bang nucleosynthesis, and wrote celebrated popular books (*One, Two, Three... Infinity*, the Mr Tompkins series). The liquid-drop model of nuclear binding is one of his lasting contributions to nuclear physics.

Historical note: Carl Friedrich von Weizsäcker (1912–2007)

Carl Friedrich von Weizsäcker, German physicist and later philosopher, quantified Gamow's liquid-drop ideas in 1935 as the **semi-empirical mass formula**: binding energy written as a sum of volume, surface, Coulomb, and asymmetry contributions, with coefficients to be fixed by experiment [12]. His paper "Zur Theorie der Kernmassen" (Z. Phys. **96**, 431, 1935) established the algebraic structure still used today. He also worked on stellar energy generation (with Bethe) and, after the war, on the philosophy of science and the responsibility of scientists. In this course the SEMF is the Weizsäcker formula in modern notation, with standard numerical coefficients from global mass fits.

Historical note: Hans A. Bethe (1906–2005)

Hans Albrecht Bethe, German-American theoretical physicist, refined and popularised the mass formula in 1935 (hence *Bethe–Weizsäcker*). He received the 1967 Nobel Prize in Physics for the theory of energy production in stars (the CNO cycle and related work). Across a long career at Cornell he shaped nuclear and particle theory, nuclear astrophysics, and the theory of neutron stars. In the present lectures his name attaches both to the SEMF coefficients and to the stellar/compact-object applications of binding-energy systematics (Lectures 4–5).

1.6 SEMF terms derived in detail

The previous sections introduced the five SEMF terms and their historical origin. We now study each term in turn: packing for volume and surface, electrostatics for Coulomb, Fermi-gas (and shell) filling for asymmetry, and separation-energy systematics for pairing [13, 6, 1, 14, 2]. The A and Z dependence of each term reflects simple physical properties even though most numerical coefficients must be fitted [14].

1.7 Volume term: why $B_V = a_V A$

The volume term is the backbone of the B/A curve. If it were the only contribution, every nucleus would have $B/A = a_V \sim 15$–$16\,\mathrm{MeV}$ independent of A and Z. All other SEMF terms are corrections that pull the actual curve away from that flat ceiling.

1.7.1 Short-range force and nearest-neighbour counting

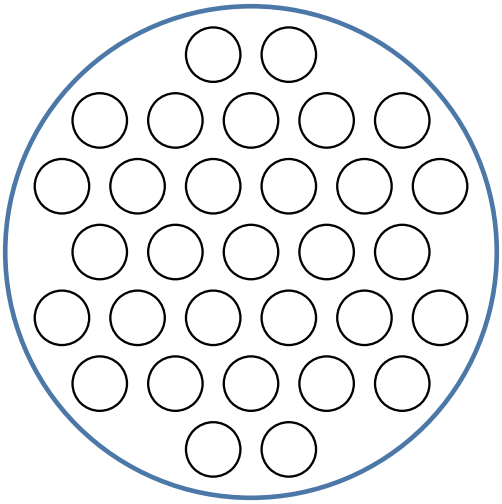

Figure 1.3: Volume (interior) nucleon. The open central circle is fully surrounded; black arrows show short-range attractive bonds to nearest neighbours (red).

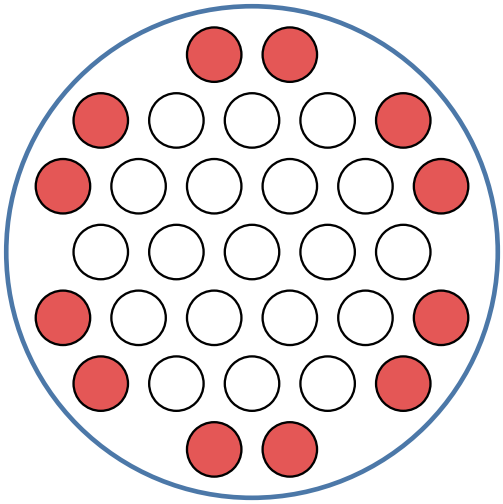

Figure 1.4: Surface nucleons (red). Some neighbour directions point outside the nucleus. Missing bonds reduce the binding energy.

Step 1 (range). The residual strong force has range $\sim$ 1–2 fm, comparable to the mean nucleon spacing but much smaller than the radius of a heavy nucleus. Therefore an interior nucleon interacts only with a fixed number of nearest neighbours, not with all other $A-1$ nucleons [6, 1, 13, 2].

Step 2 (saturated density). Electron scattering shows that the central density is nearly independent of A. Each interior nucleon therefore has roughly the *same* number of neighbours, call it n_{nn} (order ten). Constant nucleon density likewise implies $V \propto A$ and a binding contribution proportional to A for medium-to-heavy nuclei [2].

Step 3 (bond sharing). Let $U > 0$ be the attractive energy associated with one nearest-neighbour bond. Each bond is shared by two nucleons, so the contribution of bonds to the binding energy of one interior nucleon is

$$\frac{B}{A}\Big|_{\mathrm{bulk}} \approx \frac{1}{2}\, n_{\mathrm{nn}}\, U. \tag{1.24}$$

For A nucleons,

$$B_V = a_V\, A, \qquad a_V \equiv \tfrac{1}{2}\, n_{\mathrm{nn}}\, U. \tag{1.25}$$

Equivalently, without bond counting: nucleons are closely packed and the force is short ranged, so each nucleon contributes in the same way independently of the total number; the force is therefore proportional to A, not to $A(A-1)/2 \sim A^2$ [13].

In three-dimensional close packing of equal spheres, $n_{\mathrm{nn}} = 12$, so $a_V = 6U$. Fitting nuclear masses gives

$$a_V \approx 15.5\text{–}15.8\,\mathrm{MeV} \tag{1.26}$$

[6, 1, 14, 13], hence a pedagogical bond scale $U \sim a_V/6 \sim 2.6\,\mathrm{MeV}$. That U is an effective

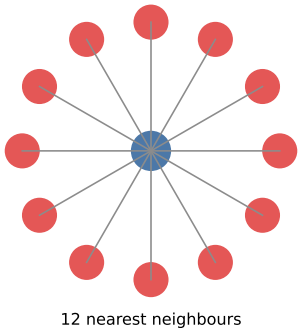

Figure 1.5: Idealised close packing: a central nucleon with twelve nearest neighbours (fcc/hcp coordination number 12).

number after kinetic energy is subtracted (see below), not a bare NN potential depth. By itself the volume term would give a flat $B/A \sim 16\,\text{MeV}$; all other SEMF terms reduce that ceiling toward the observed $\sim 8\,\text{MeV}$ [14].

1.7.2 Why not A^2? (long-range would fail)

If every nucleon attracted every other, the number of pairs would be

$$\binom{A}{2} = \frac{A(A-1)}{2} \propto A^2, \tag{1.27}$$

so $B \propto A^2$ and $B/A \propto A$. Experiment shows B/A is nearly flat ($\sim 8\,\text{MeV}$) for medium-heavy nuclei. That single fact forces nearest-neighbour (volume) scaling and rules out long-range counting for the strong force [6, 1].

Checklist for the volume term

1. Force range $\ll R \Rightarrow$ only nearest neighbours.
2. Constant density $\Rightarrow$ fixed coordination number.
3. $B_V = a_V A$ (linear in A, not A^2).
4. a_V is the largest SEMF coefficient: bulk attraction sets the energy scale.

1.7.3 Why $a_V \sim 16\,\text{MeV}$, not $\sim 50\,\text{MeV}$

Scattering and few-body work suggest that the potential energy of a nucleon in nuclear matter is of order $U_{\text{pot}} \sim -40$ to $-50\,\text{MeV}$. The SEMF volume coefficient is much smaller. The resolution is that the fitted $a_V \approx 15.5\,\text{MeV}$ is smaller than the binding of a nucleon to its neighbours inferred from the strength of the nuclear interaction ($\sim 50\,\text{MeV}$): the total binding is the difference between that attraction and the kinetic energy of the nucleon itself [13]. Nucleons are fermions and fill Fermi levels up to $\varepsilon_F \sim 35\,\text{MeV}$. The mean kinetic energy per nucleon is $\frac{3}{5}\varepsilon_F \sim 21\,\text{MeV}$. The *net* volume binding is

$$a_V \sim |U_{\text{pot}}| - \tfrac{3}{5}\varepsilon_F \sim 15\text{–}20\,\text{MeV}, \tag{1.28}$$

in agreement with the fitted a_V [13, 14]. Thus a_V already encodes the competition between short-range attraction and Fermi kinetic energy. A mean-potential estimate that yields $\sim 8\,\mathrm{MeV}$ per nucleon after filling oscillator shells is the same physics in a shell-model language [14].

1.8 Surface term: why $-a_S A^{2/3}$

The surface term explains why B/A is *low* for the lightest nuclei and rises toward mid-mass (Section 1.4.2). Interior nucleons are fully coordinated; surface nucleons miss outward-pointing bonds. At small A almost every nucleon is a surface nucleon, so the fractional penalty $|B_S|/A \propto A^{-1/3}$ is large.

Step 1. Not every nucleon is an interior nucleon. Those on the surface (Figure 1.4) have fewer neighbours and are less tightly bound [1, 6, 13, 4]. In liquid-drop language: internal nucleons feel isotropic interactions, whereas nucleons near the surface feel forces coming only from the inside; the correction is therefore a surface-tension term [14]. Surface nucleons experience a smaller force, so the term is negative [4].

Step 2. Constant density $\Rightarrow R = r_0 A^{1/3}$. The surface area of a sphere is

$$S = 4\pi R^2 = 4\pi r_0^2\, A^{2/3} \propto A^{2/3}. \tag{1.29}$$

Equivalently, $S \propto V^{2/3}$ for a spherical nucleus [1]. The number of under-bound surface nucleons therefore scales as $A^{2/3}$.

Step 3. The volume term $a_V A$ *overcounts* the binding of surface nucleons (it pretends they have a full set of neighbours). One must subtract a correction proportional to the surface area:

$$B_S = -\,a_S\, A^{2/3}, \qquad a_S \approx 16.8\text{–}17.8\,\mathrm{MeV}. \tag{1.30}$$

The coefficient a_S is of the same order as a_V, as expected if both come from the same short-range bonds; empirically $a_S \sim 13$–$18\,\mathrm{MeV}$ [13, 14]. Together with Coulomb, the surface term limits the maximum A for which stable nuclei can exist: surface tension is literally what gives the model its name [5].

Effect on B/A.

$$\frac{B_S}{A} = -\frac{a_S}{A^{1/3}}. \tag{1.31}$$

At small A, almost all nucleons are on the surface, so B/A is strongly reduced. As A grows, surface/volume $\propto A^{-1/3}$ falls and B/A rises toward the volume ceiling. That is the main reason the experimental binding curve climbs through the light nuclei (Figure 1.10).

After volume and surface alone,

$$B \approx a_V A - a_S A^{2/3}. \tag{1.32}$$

Equation (1.32) depends only on A. It cannot explain Z dependence, the fall of B/A past iron, or the valley of stability. Three more terms are required.

Remark

A Fermi-gas treatment of kinetic energy in a finite box also produces a surface piece $\propto A^{2/3}$ (missing states near free surfaces). The empirical a_S combines that kinetic surface correction with the missing-bond (potential) surface tension [14].

1.9 Coulomb term: why $-a_C Z(Z-1)/A^{1/3}$

Unlike the nuclear force, Coulomb repulsion is long range: every proton feels every other proton. That is why the Coulomb piece scales as $Z(Z-1)$, not as Z. It is also the main reason B/A *falls* slowly past the iron peak (Section 1.4.2) and why heavy stable nuclei need a neutron excess to dilute the proton charge [1, 6, 13, 2]. Basic electrostatics gives a potential energy for a uniform spherical distribution of Z charges proportional to $Z(Z-1)/R$; with $R \propto A^{1/3}$ this becomes the familiar SEMF Coulomb term [1]. The analytic coefficient for a sharp sphere with $r_0 = 1.2\,\text{fm}$ is $a_C = 0.72\,\text{MeV}$; one often still leaves a_C slightly free because the real charge density is diffuse near the nuclear surface [1, 6].

1.9.1 Combinatorial count of proton pairs

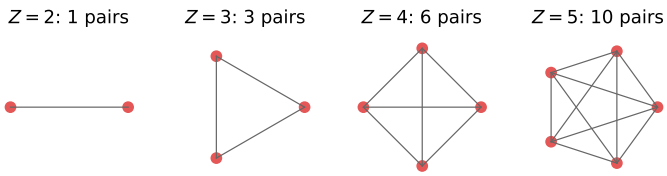

Figure 1.6: Pairwise interactions among Z protons: 2 protons $\to$ 1 link; 3 $\to$ 3; 4 $\to$ 6; 5 $\to$ 10. In general $\binom{Z}{2} = Z(Z-1)/2$. Because Coulomb is long range, every pair contributes.

Step 1 (long range). Number of distinct pp pairs:

$$\frac{Z(Z-1)}{2}. \tag{1.33}$$

Using $Z(Z-1)$ rather than Z^2 avoids counting a proton's self-repulsion [1, 6].

Step 2 (distance scale). Typical inter-proton distances scale with the nuclear radius $R \propto A^{1/3}$. Hence the Coulomb energy scales as

$$E_C \propto \frac{Z(Z-1)}{R} \propto \frac{Z(Z-1)}{A^{1/3}}. \tag{1.34}$$

1.9.2 Continuum formula: the factor $3/5$

A controlled calculation treats the nucleus as a uniformly charged sphere of charge Ze and radius R. Assemble the sphere by bringing in thin charged shells from infinity.

At intermediate radius $r \le R$, the charge already present is

$$q(r) = Ze\,\frac{r^3}{R^3}, \tag{1.35}$$

and the potential at the surface of that sphere is $q(r)/(4\pi\varepsilon_0 r)$. The work to add a shell of charge $\mathrm{d}q = Ze \cdot 3r^2\,\mathrm{d}r/R^3$ is

$$\mathrm{d}W = \frac{q(r)}{4\pi\varepsilon_0 r}\,\mathrm{d}q = \frac{1}{4\pi\varepsilon_0}\frac{Ze\,r^2}{R^3}\cdot Ze\cdot\frac{3r^2}{R^3}\,\mathrm{d}r = \frac{(Ze)^2}{4\pi\varepsilon_0}\frac{3r^4}{R^6}\,\mathrm{d}r. \tag{1.36}$$

Integrating from $r = 0$ to $r = R$,

$$\begin{aligned} E_C &= \frac{(Ze)^2}{4\pi\varepsilon_0}\frac{3}{R^6}\int_0^R r^4\,\mathrm{d}r = \frac{(Ze)^2}{4\pi\varepsilon_0}\frac{3}{R^6}\cdot\frac{R^5}{5} \\ &= \frac{3}{5}\frac{1}{4\pi\varepsilon_0}\frac{(Ze)^2}{R}. \end{aligned} \tag{1.37}$$

(The factor 3/5 is pure geometry of a uniform sphere [13, 2, 1].)

With $R = r_0 A^{1/3}$ and $r_0 \approx 1.2\,\mathrm{fm}$,

$$\begin{aligned} a_C &= \frac{3}{5}\frac{e^2}{4\pi\varepsilon_0\, r_0} = \frac{3}{5}\frac{\hbar c\,\alpha}{r_0} \\ &\approx \frac{3}{5}\frac{197\,\mathrm{MeV\,fm}\times 1/137}{1.2\,\mathrm{fm}} \approx 0.72\,\mathrm{MeV}. \end{aligned} \tag{1.38}$$

In the SEMF one usually keeps the discrete-pair refinement

$$B_C = -\,a_C\,\frac{Z(Z-1)}{A^{1/3}}, \qquad a_C \approx 0.71\text{–}0.72\,\mathrm{MeV}. \tag{1.39}$$

(Replacing Z^2 by $Z(Z-1)$ subtracts the spurious self-energy of each proton.) Fits often leave a_C slightly free because the real charge density is not a sharp uniform sphere [1].

Physics consequences.

- $B_C < 0$: Coulomb always reduces binding relative to pure strong attraction.
- Along the valley, $Z \sim A/2$ to $A/2.5$, so $|B_C|/A$ grows roughly as $A^{2/3}$. That drives the slow *decline* of B/A for heavy nuclei.
- Coulomb alone favours $Z \to 0$ at fixed A. Nature does not: the asymmetry term restores $N \sim Z$.

Example: Coulomb cost for heavy nuclei

For $A \sim 238$, $Z \sim 92$,

$$\frac{B_C}{A} \sim -0.72\cdot\frac{92\cdot 91}{238^{4/3}} \approx -4.1\,\mathrm{MeV},$$

a multi-MeV reduction of B/A compared with a light nucleus. Volume and surface alone cannot produce that heavy-end decline.

After volume, surface and Coulomb,

$$B = a_V A - a_S A^{2/3} - a_C\frac{Z(Z-1)}{A^{1/3}}. \tag{1.40}$$

Maximising B at fixed A still pushes $Z \to 0$. The next term stops that pathology.

1.10 Valley of stability: what Coulomb + asymmetry must explain

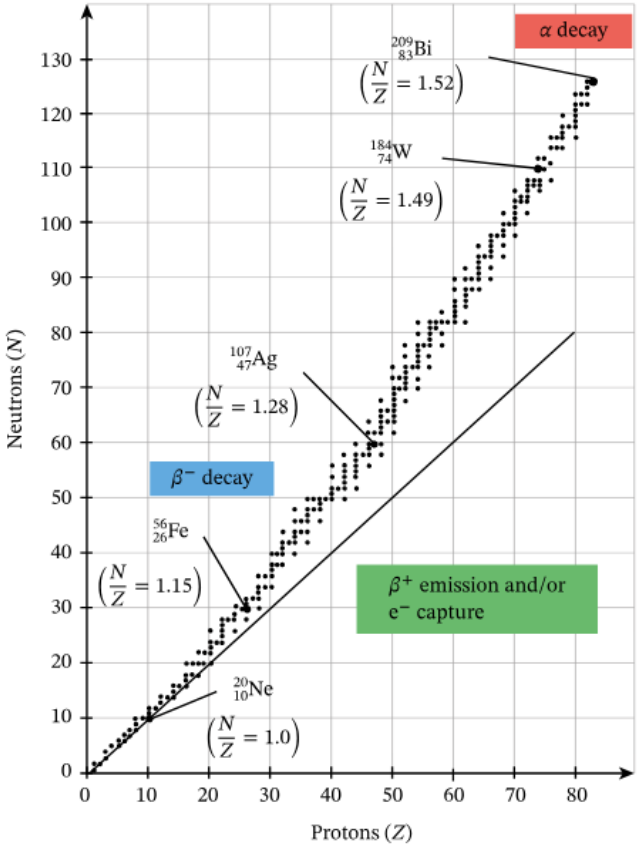

Figure 1.7: Chart of β-stable nuclides in the N–Z plane. Light systems hug $N = Z$. Heavier systems drift to $N > Z$ ($N/Z \approx 1.15$ for Fe, ≈ 1.28 for Ag, ≈ 1.49 for W, ≈ 1.52 for Bi). Neutron-rich: β^-. Proton-rich: β^+ / EC. Very heavy: α decay.

Figure 1.7 is the experimental map that Coulomb and asymmetry must jointly explain [6, 1, 13, 5, 14]:

1. **Light nuclei, $N \approx Z$.** Nuclear force is (approximately) charge independent. Pauli filling of two Fermi seas then prefers equal proton and neutron numbers when Coulomb is still weak. On the Segrè chart, stable nuclides hug $N \approx Z$ for $Z \lesssim 20$ [5].

2. **Heavy nuclei, $N > Z$.** Coulomb $\propto Z^2/A^{1/3}$ grows with Z. Extra neutrons dilute the proton density without adding Coulomb cost, so the valley bends above the $N = Z$ line ($N/Z \approx 1.15$ for Fe, ≈ 1.5 near Bi). Without an asymmetry term the SEMF would allow "stable isotopes of hydrogen with hundreds of neutrons" [6].

3. **Decay regions.** Neutron rich $\Rightarrow \beta^-$; proton rich $\Rightarrow \beta^+$ or EC. Very heavy systems also α decay when Coulomb has lowered B/A enough.

Without the asymmetry term, volume and surface alone place no restriction on N/Z, while Coulomb alone would drive every isobar toward $Z \to 0$. Nature does neither: the next term restores $N \sim Z$ at small A and permits only a controlled neutron excess at large A [1, 13].

Key idea

The valley is not a separate SEMF term. It is the observable balance of Coulomb (wants fewer protons) against asymmetry (wants $N = Z$).

1.11 Asymmetry (symmetry) term: why $-a_{\mathrm{a}}(N-Z)^2/A$

Volume, surface, and Coulomb would allow any N/Z ratio at fixed A. Coulomb alone would drive $Z \to 0$. The asymmetry term restores $N \approx Z$ when Coulomb is weak and permits only a *controlled* neutron excess when Coulomb is strong. Together with Coulomb it shapes the valley of stability (Figure 1.7) and the mass parabolas of Lecture 5.

1.11.1 Physical picture

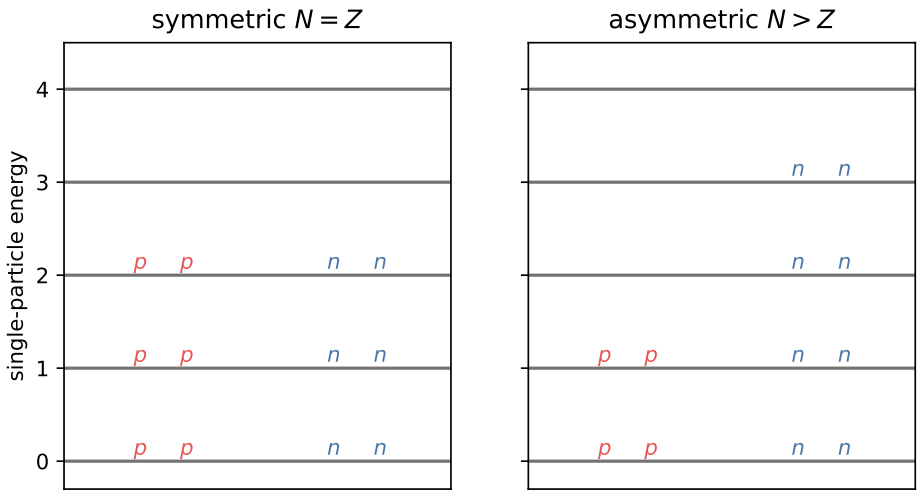

Figure 1.8: Left: symmetric filling $Z = N = A/2$. Right: asymmetric filling with extra neutrons. Excess neutrons must occupy higher single-particle levels, raising the total kinetic energy and lowering B.

Protons and neutrons are distinct fermions. Each species fills its own ladder of single-particle levels (Pauli principle) [6, 13, 14, 2, 4].

- If $N = Z$, both ladders are filled to the same height: minimal kinetic energy for given A.
- If $N > Z$, the neutron ladder is filled higher and the proton ladder lower. The extra neutrons sit in higher orbitals, so the total kinetic energy rises even though A is fixed.
- Higher energy of the system $\Rightarrow$ *smaller* binding energy B.

You cannot put excess neutrons into empty low proton levels: they are different particles. This correction (and pairing) go beyond a purely classical liquid drop: they require the quantum exclusion principle and, ultimately, the shell model [13]. A simple shell-level cartoon makes the scaling plausible: if adjacent shells are spaced by a constant δ, moving a proton up into a neutron orbital costs an energy that grows with the imbalance and yields the form $(N-Z)^2/A$ after averaging [4]. The same quadratic form follows from two Fermi gases (next subsection) [2].

1.11.2 Scaling: why $(N-Z)^2/A$

Define the neutron excess

$$\Delta \equiv N - Z = A - 2Z. \tag{1.41}$$

Two independent arguments give the same functional form.

(A) Toy ladder with spacing δ. Move $\Delta/2$ nucleons from the proton sea to the neutron sea. Each moved nucleon is raised by an energy of order $\delta \cdot (\Delta/2)$ relative to the Fermi surface, so the excess energy scales as

$$\Delta E \sim \delta \cdot \frac{\Delta^2}{4}. \tag{1.42}$$

In a large system the level density near the Fermi surface grows with A, so $\delta \sim 1/A$. Therefore

$$\Delta E \propto \frac{(N-Z)^2}{A}. \tag{1.43}$$

(B) Two Fermi gases (standard derivation). Let protons and neutrons be free Fermi gases in volume $V \propto A$, densities $\rho_p = Z/V$, $\rho_n = N/V$. The kinetic energy of one species is

$$E_{\mathrm{kin},\tau} = \frac{3}{5} N_\tau \frac{\hbar^2}{2m} (3\pi^2 \rho_\tau)^{2/3} = \frac{3}{5} N_\tau \, \varepsilon_{F,\tau}. \tag{1.44}$$

Write $N = (A/2)(1+x)$, $Z = (A/2)(1-x)$ with $x = (N-Z)/A = \Delta/A$. Because $\varepsilon_{F,\tau} \propto \rho_\tau^{2/3} \propto N_\tau^{2/3}$,

$$E_{\mathrm{kin}} = C' \left[\left(\frac{A}{2}\right)^{5/3} (1+x)^{5/3} + \left(\frac{A}{2}\right)^{5/3} (1-x)^{5/3} \right],$$

with C' fixed by the saturation Fermi energy. Expand $(1 \pm x)^{5/3} = 1 \pm \frac{5}{3}x + \frac{5}{9}x^2 + \cdots$: the odd powers cancel and

$$\begin{aligned} E_{\mathrm{kin}} &= 2C' \left(\frac{A}{2}\right)^{5/3} \left(1 + \frac{5}{9}x^2 + \cdots\right) \\ &= CA + \frac{C}{3} \frac{(N-Z)^2}{A} + \cdots, \end{aligned} \tag{1.45}$$

with $C = \frac{3}{5}\varepsilon_F$ at $N = Z$ ($\varepsilon_F \approx 35\,\mathrm{MeV}$ at saturation density). The linear (volume) piece is absorbed into a_V. The quadratic piece *raises* the energy of the nucleus and therefore *lowers* the binding:

$$B_{\mathrm{a}} = -\, a_{\mathrm{a}} \frac{(N-Z)^2}{A} = -\, a_{\mathrm{a}} \frac{(A-2Z)^2}{A}. \tag{1.46}$$

Empirical fits give

$$a_{\mathrm{a}} \approx 23\text{–}24\,\mathrm{MeV} \tag{1.47}$$

[6, 1, 14]. The pure kinetic estimate $C/3 \sim \varepsilon_F/3 \sim 12\,\mathrm{MeV}$ is only about half of the empirical value: the rest comes from isovector potential energy (the force also prefers $N = Z$). The *form* $(N-Z)^2/A$ is already fixed by the Fermi gas.

Caution

Some modern fits write $-a'(Z - A/2)^2/A$ with $a' \approx 94\,\text{MeV}$. Because $(Z - A/2)^2 = (N - Z)^2/4$, that is the same physics with a coefficient four times larger. Always check the algebraic form before copying a number [4].

Checklist for the asymmetry term

1. Vanishes when $N = Z$.
2. Grows as $(N - Z)^2$: quadratic cost of imbalance.
3. Falls as $1/A$: large systems tolerate imbalance more easily (so heavy nuclei can sit at $N > Z$).
4. Together with Coulomb, fixes N/Z along Figure 1.7.

Key idea

Asymmetry energy is mainly a kinetic (Pauli) penalty, reinforced by isovector mean fields. It is not a new fundamental force. Figure 1.8 is the picture to keep: extra neutrons climb the neutron ladder.

After Coulomb and asymmetry,

$$B = a_V A - a_S A^{2/3} - a_C \frac{Z(Z-1)}{A^{1/3}} - a_\text{a} \frac{(N-Z)^2}{A}. \tag{1.48}$$

1.11.3 Most stable Z at fixed A (preview; full derivation in Lecture 5)

Ignore pairing, treat A fixed, and minimise the atomic mass (or maximise B) with respect to Z. Balancing Coulomb against asymmetry yields the schematic result

$$Z^* \approx \frac{A/2}{1 + \kappa A^{2/3}}, \qquad \kappa \sim \frac{a_C}{4a_\text{a}} \approx 0.0075, \tag{1.49}$$

so $Z^* \approx A/2$ for light nuclei and $Z^* < A/2$ ($N > Z$) for heavy ones: the bend of Figure 1.7 [14, 1, 6, 13]. The same stationarity condition is the Z_min formula that Lecture 5 will derive carefully, including the small $m_n - m(^1\text{H})$ shift [6].

Remark

Lecture 5 starts from $M(A, Z)$, differentiates carefully with respect to Z (including $m_n - m(^1\text{H})$), obtains the working formula $Z \approx A/[2(1 + 0.0078\,A^{2/3})]$, and connects that minimum to mass-parabola figures for odd and even A.

1.12 Pairing term: why δ depends on even/odd N, Z

Pairing is the smallest of the five SEMF terms in magnitude (typically $\sim 1\,\text{MeV}$ total, or $\lesssim 0.1\,\text{MeV}$ per nucleon), but it has outsized consequences for stability. It produces the odd–even

staggering on B/A and, at fixed even A, splits the mass surface into two parabolas in Lecture 5.

1.12.1 Physical idea

Like nucleons (two protons or two neutrons) tend to form $J = 0$ pairs (opposite angular momenta). A paired configuration lies lower than an unpaired occupancy of the last orbital [6, 1, 13, 2]. Hence:

- even N (or Z): pairs complete $\Rightarrow$ extra binding;
- odd N (or Z): one unpaired nucleon $\Rightarrow$ less binding.

The odd–odd case is especially clear: when both Z and N are odd, one gains binding by converting one of the odd protons into a neutron (or vice versa) so that it can form a pair with its formerly odd partner [6]. With all other factors fixed, one must therefore *subtract* from B for odd–odd configurations and *add* for even–even ones [13]. Equivalently, two protons (or two neutrons) can occupy the same orbital with opposite spins, while an odd–odd nucleus always has an unpaired nucleon forced into the next higher level [2].

1.12.2 Experimental evidence: separation energies

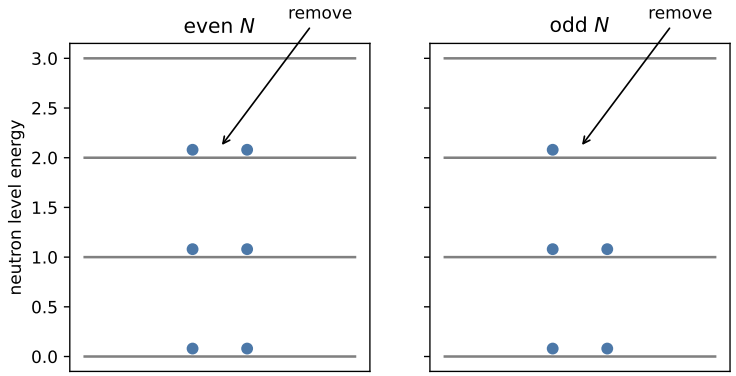

Figure 1.9: Schematic neutron separation: energy cost S_n. Even N: a pair must be broken. Odd N: the unpaired neutron is cheaper to remove.

$$S_n(A, Z) = [M(A-1, Z) + m_n - M(A, Z)]c^2, \tag{1.50}$$

$$S_p(A, Z) = [M(A-1, Z-1) + m_p - M(A, Z)]c^2. \tag{1.51}$$

Plotting S_n versus N shows a sawtooth: S_n is larger for even N (break a pair) than for odd N (remove the unpaired neutron). The same stagger appears in S_p versus Z [6, 1].

1.12.3 Census of stable nuclei

Configuration	Approx. number of β-stable nuclides
Even–even (Z even, N even)	$\sim$ 165–167
Odd A (exactly one of Z, N odd)	$\sim$ 100–110
Odd–odd (Z and N both odd)	only 4 (light)

The four stable odd–odd nuclei are ^{2}H, ^{6}Li, ^{10}B, and ^{14}N [6, 1]. Heavier odd–odd systems almost always β decay so that the unpaired proton and neutron become a like pair in an even–even daughter.

1.12.4 Pairing term in the SEMF

Taking odd-A nuclei as the baseline,

$$\delta = \begin{cases} +\,a_P\,A^{-3/4} & \text{even–even (more bound)}, \\ 0 & \text{odd } A, \\ -\,a_P\,A^{-3/4} & \text{odd–odd (less bound)}. \end{cases} \tag{1.52}$$

Throughout Lectures 4–5 we use the single convention $a_P = 34\,\text{MeV}$ with $A^{-3/4}$. Other texts may instead use $\sim 12\,A^{-1/2}\,\text{MeV}$; coefficients from those two conventions must never be interchanged [6, 1, 14, 2].

Caution

Sign conventions differ between sources (some write δ with the opposite overall sign in B vs M). Always verify that even–even nuclei gain binding and odd–odd nuclei lose it, and check whether a given formula fits B or M [1].

1.13 The full Weizsäcker / Bethe–Weizsäcker formula

Semi-empirical mass formula

$$B(A,Z) = a_V A - a_S A^{2/3} - a_C \frac{Z(Z-1)}{A^{1/3}} - a_{\mathrm{a}} \frac{(N-Z)^2}{A} + \delta, \tag{1.53}$$

with $N = A - Z$ and δ from Equation (1.52).

Equivalently, in atomic-mass form [4, 5, 6],

$$m(A,Z) = Z\,m(^{1}\mathrm{H}) + N\,m_n - B(A,Z)/c^2, \tag{1.54}$$

which connects the SEMF directly to tabulated masses. The Coulomb piece is sometimes written as $a_C Z^2/A^{1/3}$ (the large-Z approximation to $Z(Z-1)$); we keep $Z(Z-1)$ in (1.53) [14, 1, 6].

Coeff.	Typical value	Role	Derivation key
a_V	15.5–15.8 MeV	bulk nearest-neighbour net attraction	short range + saturation; net of Fermi KE
a_S	16.8–17.8 MeV	missing surface bonds	$S \propto R^2 \propto A^{2/3}$
a_C	≈ 0.72 MeV	proton self-energy	pairs $Z(Z-1)/2$; sphere 3/5
a_{a}	23–24 MeV	$N \neq Z$ kinetic (+ potential) penalty	two Fermi gases $\Rightarrow (N-Z)^2/A$
a_P	12–34 MeV	even–odd pairing	S_n stagger; even–even preference

A standard coefficient set that reproduces B/A well is [6, 1]

$$\begin{aligned} a_V &= 15.5\,\text{MeV}, \quad a_S = 16.8\,\text{MeV}, \qquad\qquad a_C = 0.72\,\text{MeV}, \\ a_\text{a} &= 23\,\text{MeV}, \qquad a_P = 34\,\text{MeV} \qquad (\text{with } A^{-3/4}). \end{aligned} \tag{1.55}$$

Other widely used fits give $a_V = 15.75$, $a_S = 17.8$, $a_C = 0.71$, $a_\text{a} = 23.7\,\text{MeV}$ [14], or nearly the same numbers (15.76, 17.81, 0.711, 23.7) [5], or $a_V \approx 15.8$, $a_S \approx 18.3$, $a_C \approx 0.71$ with pairing $\sim A^{-1/2}$ [4]. Differences of a few percent are fit choices (mass range, shell nuclei included or not), not new physics.

Remark

The SEMF is semi-empirical: the *forms* come from physics; the *numbers* are fixed by global fits to measured masses. It does not replace the shell model for magic numbers and spectroscopy, but it organises the bulk of the binding curve [6, 1]. Its importance is not that it predicts exotic new phenomena, but that it is a first successful application of nuclear models to a systematic nuclear property [6].

1.14 How the terms stack on B/A

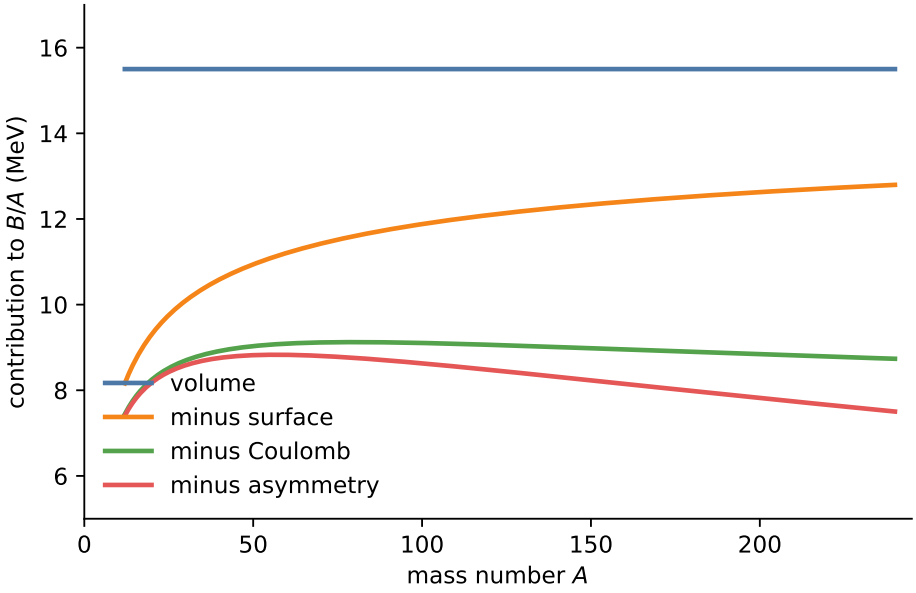

Figure 1.10: Decomposition of mean binding energy per nucleon. Top: volume ceiling. Subtract surface: rising light-A side. Subtract Coulomb: downward bend at large A. Asymmetry removes a further slice for neutron-rich heavy systems. Red: net B/A (pairing not drawn).

Read Figure 1.10 from the top down at fixed A [2, 1, 13]:

How to read the B/A stack

1. **Volume (top).** Flat near $a_V \sim 15$–$16\,\text{MeV}$. Independent of A if density and coordination number are fixed.

2. **Minus surface.** Large at small A; shrinks as $A^{-1/3}$. Explains the *rise* of net B/A from light nuclei toward iron.
3. **Minus Coulomb.** Grows with $Z^2/A^{4/3}$. Explains the *fall* of B/A past iron and the need for neutron excess.
4. **Minus asymmetry.** Extra cost when $|N - Z|$ is large. Moderate on the valley; large off it (drives β decay).
5. **Net B/A.** Peak near $A \sim 56$–62; fusion below the peak, fission above. Pairing is a small even–odd ripple on top.

Numerical sketch: ^{56}Fe

Use $a_V = 15.5$, $a_S = 16.8$, $a_C = 0.72$, $a_\mathrm{a} = 23$ (MeV) for ^{56}Fe ($A = 56$, $Z = 26$, $N = 30$):

$$\begin{aligned}\frac{B_V}{A} &= 15.5,\\ \frac{B_S}{A} &= -\frac{16.8}{56^{1/3}} \approx -4.4,\\ \frac{B_C}{A} &= -0.72 \cdot \frac{26 \cdot 25}{56^{4/3}} \approx -2.18,\\ \frac{B_\mathrm{a}}{A} &= -23 \cdot \frac{(4)^2}{56^2} \approx -0.12.\end{aligned}$$

Sum ≈ 8.8 MeV before pairing: the right order of magnitude compared with the experimental peak near 8.8 MeV. Coefficients are global fits, not exact for every nuclide.

Worked stacking: ^{100}Mo and ^{208}Pb

Take the same coefficients and valley charges $Z \approx A/[2(1 + 0.0078A^{2/3})]$: for $A = 100$, $Z \approx 43$; for $A = 208$, $Z \approx 82$.

Medium mass (^{100}Mo, $Z = 42$ for the stable isobar):

$$\frac{B_V}{A} = 15.5, \quad \frac{B_S}{A} = -\frac{16.8}{100^{1/3}} \approx -3.6, \quad \frac{B_C}{A} \approx -0.72 \cdot \frac{42 \cdot 41}{100^{4/3}} \approx -2.67,$$

$$\frac{B_\mathrm{a}}{A} \approx -23 \cdot \frac{16^2}{100^2} \approx -0.59 \quad \Rightarrow \quad B/A \approx 8.62\,\mathrm{MeV}.$$

The surface penalty is already moderate; Coulomb and asymmetry together remove ~ 3.26 MeV/nucleon from the volume ceiling.

Heavy nucleus (^{208}Pb, $Z = 82$, $N = 126$):

$$\frac{B_S}{A} \approx -\frac{16.8}{208^{1/3}} \approx -2.8, \quad \frac{B_C}{A} \approx -0.72 \cdot \frac{82 \cdot 81}{208^{4/3}} \approx -3.88,$$

$$\frac{B_\mathrm{a}}{A} \approx -23 \cdot \frac{44^2}{208^2} \approx -1.03 \quad \Rightarrow \quad B/A \approx 7.75\,\mathrm{MeV} \text{ (before pairing)}.$$

Surface is a smaller fraction of A, but Coulomb and asymmetry now dominate: the net

B/A has fallen ~ 1.1 MeV below the iron peak even though the volume term is unchanged. That is the liquid-drop reason heavy nuclei are less tightly bound per nucleon and why fission can release energy by moving toward mid-mass daughters.

Vertical slices at small and large A

At $A \sim 20$: surface slice is thick; Coulomb slice is thin; net B/A still climbing.
At $A \sim 200$: surface slice is thinner; Coulomb slice is thick; asymmetry is visible; net B/A has fallen below the iron maximum.
That is the physics of stellar fusion (building toward iron) and of fission reactors (splitting uranium toward the peak).

1.15 Term-by-term derivation summary

Term	Form	Why that form
Volume	$+a_V A$	short range + fixed neighbours $\Rightarrow$ linear in A, not A^2; net of Fermi KE.
Surface	$-a_S A^{2/3}$	surface nucleons under-bound; $S \propto R^2 \propto A^{2/3}$.
Coulomb	$-a_C Z(Z-1)/A^{1/3}$	long-range pairs $Z(Z-1)/2$; $R \propto A^{1/3}$; sphere factor 3/5.
Asymmetry	$-a_{\mathrm{a}}(N-Z)^2/A$	two Fermi seas; expand E_{kin} for $N \neq Z$; $\delta \sim 1/A$.
Pairing	$\delta(\mathrm{ee}/A/\mathrm{oo})$	like-nucleon pairs; S_n stagger; almost no stable odd–odd.

1.16 Deeper physics: SEMF coefficients and the B/A landscape

1.16.1 Standard coefficient sets

Fitting the liquid-drop formula to measured masses yields coefficient sets that agree at the 10% level. One convenient set is [1]

Coefficient	Typical value (MeV)	Role
a_V	15.5	volume attraction
a_S	16.8	surface deficit
a_C	0.72	Coulomb (3/5 sphere)
a_{a}	23.2	asymmetry / symmetry
a_P	34	pairing ($\pm A^{-3/4}$ or $\pm A^{-1/2}$)

A modern alternative quotes $a_V \approx 15.8$, $a_S \approx 18.3$, $a_C \approx 0.71$, $a_a \approx 23.2$–94.8 depending on the exact $(N-Z)^2/A$ normalisation, and $a_P \approx 11$–12 MeV for an $A^{-1/2}$ pairing form [4]. One derives

$a_C = 3e^2/(5 \cdot 4\pi\varepsilon_0 r_0)$ from the uniform-sphere Coulomb integral and recovers $a_C \sim 0.7\,\text{MeV}$ for $r_0 \sim 1.2\,\text{fm}$.

Caution

Coefficients are *fit parameters* to terrestrial masses near the valley of stability. Using them far from stability (drip lines) or at extreme A (neutron stars) is an extrapolation: useful for orientation, not a substitute for a microscopic EOS.

1.16.2 Features of the B/A curve that the SEMF must reproduce

1. **Rise at low A:** surface term $\propto A^{-1/3}$ dominates; light nuclei are surface-rich.
2. **Broad maximum near $A \sim 56$–62** (iron–nickel): competition of surface (wants larger A) and Coulomb (wants smaller Z, hence limits growth).
3. **Slow decline for heavy A:** Coulomb $\propto Z^2/A^{1/3}$ grows; fission becomes favourable.
4. **Odd–even staggering:** pairing; even–even nuclei sit higher in B/A.
5. **Light $A = 4n$ peaks:** α-clustering (^{4}He, ^{12}C, ^{16}O) exceeds the smooth SEMF; shell and cluster physics beyond the liquid drop [2, 6].

1.16.3 Mass defect and Q values

Any reaction or decay Q value is a difference of binding energies (or masses). Fusion of light nuclei and fission of heavy nuclei both move the system toward the iron peak and release energy:

$$Q = [B(\text{products}) - B(\text{reactants})] > 0 \tag{1.56}$$

when the products lie higher on the B/A curve. The SEMF thus organises not only stability but also the energetics of reactors and stars [1, 4].

1.17 Physics depth: SEMF term scales and competition

The liquid-drop SEMF writes

$$B = a_V A - a_S A^{2/3} - a_C \frac{Z(Z-1)}{A^{1/3}} - a_a \frac{(A-2Z)^2}{A} + \delta, \tag{1.57}$$

with typical magnitudes $a_V \sim 16\,\text{MeV}$, $a_S \sim 18\,\text{MeV}$, $a_C \sim 0.7\,\text{MeV}$, $a_a \sim 23\,\text{MeV}$. Each term has a distinct A, Z scaling that students should feel numerically, not only symbolically.

1.17.1 Worked estimate: Coulomb vs surface for $A = 120$

Take $Z = 50$. Then

$$E_C \sim a_C Z^2/A^{1/3} \simeq 0.7 \times 2500/4.9 \simeq 360\,\text{MeV},$$

while $E_S \sim a_S A^{2/3} \simeq 18 \times 24 \simeq 430\,\text{MeV}$. Volume binding $a_V A \sim 1920\,\text{MeV}$ still dominates, but Coulomb and surface are comparable: that near-cancellation foreshadows fission for heavier

systems (Lecture 23), where increasing Z^2/A tips the balance.

Key idea

Physical meaning of pairing δ. Pairing is a few-mega-electronvolt correction, tiny against volume binding, yet it decides even–odd mass staggering and which isobar is β-stable (Lecture 5). Microscopic pairing gaps later reappear as seniority and BCS language in the shell model.

Remark

Assumptions. The SEMF is a smooth fit. Shell gaps of several MeV near magic numbers are residuals, not failures of the idea. Extrapolating SEMF coefficients to drip lines without microscopic corrections misestimates separation energies by mega-electronvolts.

1.17.2 Competition map across the chart

For light nuclei, surface wins over Coulomb and B/A rises with A. Near $A \sim 56$, volume binding is maximised relative to the penalties, which is why the iron region is the endpoint of exothermic fusion. Beyond, Coulomb grows faster than surface decreases (relative to volume), and B/A slowly declines: fission and α decay become exothermic for the heaviest species. The SEMF is therefore a single formula that organises stellar burning, fission reactors, and α chains.

Pairing $\delta \sim 12/\sqrt{A}\,\mathrm{MeV}$ (rough scale) is negligible in absolute binding yet decisive for odd–even effects. Shell corrections of several MeV near magic numbers are the main reason global SEMF fits leave mega-electronvolt residuals: they are features to be added, not noise to be ignored.

Evaluate each SEMF term for ^{16}O, ^{56}Fe, and ^{208}Pb in a short table: the pattern of which term dominates the correction to $a_V A$ is the whole pedagogical point of the liquid-drop expansion. Coulomb in lead is already several hundred mega-electronvolts; asymmetry is smaller but decides the neutron excess. Those two sentences are the bridge from binding systematics to fission and to the valley of β stability.

Worked term-by-term table

For ^{208}Pb, evaluate volume, surface, Coulomb, and asymmetry terms with standard coefficients and verify that the sum approaches the empirical binding energy within several hundred mega-electronvolts before shell corrections. Repeat for ^{16}O and notice the surface fraction's rise. That numerical habit is the surest way to remember why each SEMF piece exists.

Physics-depth close

Term-by-term SEMF arithmetic is the fastest way to anticipate whether a process is exothermic. If you can estimate Coulomb and asymmetry changes for a proposed reaction, you already understand most of the energy budget before opening a mass table.

Physics-depth close

Term-by-term SEMF arithmetic anticipates whether a process is exothermic. Estimating Coulomb and asymmetry changes is most of the energy budget before opening a mass table.

1.18 Further physics: scales, drip lines, and limits of the SEMF

The main text derived each SEMF term. The notes below fix the *scales* of the coefficients and turn B/A into fusion, fission, and drip-line physics [6, 1, 14, 13, 2, 4, 5].

1.18.1 Coefficient sets

Coefficient	Set A	Set B	Set C
a_V (MeV)	15.5	15.75–15.76	≈ 15.8
a_S (MeV)	16.8	17.8	≈ 18.3
a_C (MeV)	0.72	0.71	≈ 0.71
a_{a} (MeV)	23	23.7	≈ 23
pairing form	$\pm a_P A^{-3/4}$	$\pm 33.6\, A^{-3/4}$	$\pm a_P A^{-1/2}$

[6, 1, 14, 5, 4]. Differences of a few percent are fit choices (which mass table, whether magic nuclei are weighted), not new physics. Always match the algebraic form of the asymmetry and pairing terms before copying a number: some fits write $(Z - A/2)^2/A$ with a coefficient four times larger than $(N - Z)^2/A$ [4, 5].

1.18.2 Fermi-gas origin of volume, surface, and asymmetry

At saturation density $n_0 \approx 0.16\,\mathrm{fm}^{-3}$ with $N \approx Z \approx A/2$ [14],

$$\varepsilon_F \approx 35\,\mathrm{MeV}, \qquad \tfrac{3}{5}\varepsilon_F \approx 21\,\mathrm{MeV}, \qquad p_F \approx 265\,\mathrm{MeV}/c. \tag{1.58}$$

A mean potential depth $U \sim -40\,\mathrm{MeV}$ then yields a net volume coefficient

$$a_V \sim |U| - \tfrac{3}{5}\varepsilon_F \sim 19\,\mathrm{MeV}, \tag{1.59}$$

close to the empirical 15–16 MeV. Expanding the kinetic energy of two Fermi gases for small $\delta = (N-Z)/A$ gives a kinetic asymmetry coefficient $\sim \varepsilon_F/3 \sim 12\,\mathrm{MeV}$; the empirical $a_{\mathrm{a}} \approx 23\,\mathrm{MeV}$ is roughly twice as large, so about half of asymmetry is potential (isovector) [14, 2].

Finite-size counting of states in a box also produces a kinetic surface term $\propto A^{2/3}$ of order 16 MeV, comparable to the empirical a_S [14]. The empirical surface coefficient therefore receives both this kinetic surface piece and the missing-bond (potential) surface tension of the liquid drop.

Thus the liquid-drop volume, surface, and asymmetry terms are not free inventions: they are the bulk, surface, and isovector pieces of a saturated Fermi liquid of nucleons.

1.18.3 Fermi-gas expansion for the asymmetry term

The kinetic energy of N_n neutrons and N_p protons in a common volume V is

$$E_K = \frac{3}{5}\,\varepsilon_F(N_n + N_p) \tag{1.60}$$

only when $N_n = N_p$. For $N_n \neq N_p$ one must use separate Fermi momenta. Setting $N_n = (A/2)(1+x)$ and $N_p = (A/2)(1-x)$ with $x = \Delta N/A$ and expanding $(1\pm x)^{5/3} = 1 \pm \frac{5}{3}x + \frac{5}{9}x^2 + \cdots$ yields [2]

$$E_K = CA + \frac{C}{3}\,\frac{(\Delta N)^2}{A} + \cdots, \tag{1.61}$$

with $C = \frac{3}{5}\varepsilon_F$ at symmetry. The first piece is absorbed into a_V; the second is precisely the asymmetry energy with a calculable kinetic coefficient. This is the derivation behind (1.46).

1.18.4 Fusion and fission Q values from B/A

Because B/A peaks near $A \sim 56$, energy is released when light nuclei fuse upward toward iron and when heavy nuclei fission downward toward iron [14, 5, 13, 6, 4]. For a reaction

$$X_1 + X_2 \to Y \qquad \text{or} \qquad X \to Y_1 + Y_2,$$

the Q value is the change in total binding energy (equivalently, the negative of the change in rest mass). The light side of the curve is the domain of stellar nuclear burning; the heavy side is the domain of fission and α decay (practically important mainly for $A \gtrsim 212$, because lifetimes are otherwise long) [14]. The SEMF, or measured mass excesses, turns the qualitative B/A argument into a number.

1.18.5 Drip lines from separation energies

Requiring the last added proton or neutron to be bound,

$$S_p > 0, \qquad S_n > 0,$$

defines the proton and neutron drip lines on the (N, Z) plane. Those lines are the boundary beyond which the last nucleon is unbound; most other combinations β or α decay toward long-lived species [14]. The SEMF predicts the drip lines semi-quantitatively; radioactive-beam experiments map the nucleus by nucleus [14, 1].

1.18.6 Pairing and mass parabolas (link to Lecture 5)

For even A, the pairing term splits the mass surface into two parabolas: even–even lower, odd–odd higher, separated by $\sim 2|\delta|$. That geometry is why some even–even nuclei can only decay by double β emission. For odd A, $\delta = 0$ and a single parabola remains [14, 6, 13, 5]. Lecture 5 makes those parabolas the main object of study.

1.18.7 What the SEMF cannot do

A few limitations should be kept in view:

- Magic numbers and shell gaps produce local spikes in B and in separation energies that the smooth SEMF misses [6, 14].
- Light $A = 4n$ cluster peaks (α, ^{12}C, ^{16}O) sit above the liquid-drop curve [2, 4].
- Coefficients fitted near the valley of stability are an extrapolation at the drip lines and a poor substitute for a microscopic EOS in neutron stars (Lecture 6) [4, 1].

The SEMF remains the right first model for the *smooth* landscape of nuclear binding.

1.19 Deeper reading: Q values from SEMF differences

Reaction and decay Q values are differences of binding energies. In the SEMF, many volume pieces cancel, leaving surface, Coulomb, and asymmetry changes as the leading drivers. That is why α decay favours heavy nuclei (large Coulomb gain for $Z \to Z - 2$) and why fusion of light nuclei releases energy while fusion of heavy nuclei does not (Lecture 25).

1.19.1 Link forward

Neutron-star crusts (Lecture 6) are assemblages of nuclei whose masses are still organised by the same SEMF bookkeeping, plus lattice and electron contributions. Rare-isotope mass measurements (Lecture 5) test how far the smooth drop formula can be trusted before shell evolution and continuum coupling dominate. When you quote a SEMF Q value, state whether pairing δ was included: for odd-A chains it can flip which neighbour is energetically favoured.

1.19.2 Fitting discipline

When students fit a_V, a_S, a_C, a_a to a mass subset, they should hold out a validation region (for example, all $A > 200$) and report the extrapolation error. Machine-learning residuals can reduce rms error on known nuclei while still failing at the drip line. The SEMF remains the right first model precisely because its failures are physically labelled: surface, Coulomb, asymmetry, pairing, and then shells.

Evaluate each SEMF term for ^{16}O, ^{56}Fe, and ^{208}Pb in a short table: the pattern of which term dominates the correction to $a_V A$ is the whole pedagogical point of the liquid-drop expansion. Coulomb in lead is already several hundred mega-electronvolts; asymmetry is smaller but decides the neutron excess. Those two sentences are the bridge from binding systematics to fission and to the valley of β stability.

SEMF checklist

Build a short table of each SEMF term for three nuclei spanning light, iron-peak, and actinide regions. Identify which correction dominates the departure from $a_V A$. Then compute one α-decay Q and one fission-rough Q from SEMF differences to preview Lectures 16 and 23. Keep pairing visible in the table even when it is numerically small.

Residual patterns

After a global SEMF fit, plot residuals versus N and Z. Magic ridges appear as systematic underbinding or overbinding corridors. Those ridges are the empirical motivation for the shell model of Lectures 12–13. Pairing residuals alternate with odd/even A. A fit that absorbs shell structure into inflated a_S or a_a will look better globally and fail locally near closures: inspect residuals before trusting extrapolations.

Astrophysical Q values

Approximate neutron-capture Q values along a chain by SEMF differences of neighbouring isotopes. Near the drip line the answers become meaningless without continuum and shell corrections, which is precisely why Lecture 5 emphasises precision masses. Use SEMF Q values only as starting guesses for network sensitivity studies.

Drop-model forecasting limits

Use a SEMF fit to predict masses for $A = 120$ (interpolation) and for a neutron-rich $A = 120$ isotope far from stability (extrapolation). Compare with AME or a microscopic mass model. The interpolation error is small; the extrapolation error can be mega-electronvolts. That contrast is the practical justification for rare-isotope mass programmes emphasised in Lecture 5 and for not using SEMF alone in r-process networks.

The SEMF's lasting value is not millimetric mass accuracy; it is a labelled decomposition of binding into volume, surface, Coulomb, asymmetry, and pairing. Every later chapter that quotes a Q value is silently using that decomposition or a microscopic correction to it.

In practice, rework one numerical estimate from the lecture with a different parameter set and compare the shift to the quoted experimental uncertainty. If the shift exceeds the uncertainty, the estimate is teaching a scale, not delivering a fit. That distinction keeps theoretical cartoons honest when they sit beside evaluated data tables and modern many-body calculations. Along the course arc, write one sentence linking this chapter backward and one forward: the discipline of those two sentences is as important as any single formula. Examination problems rarely ask for a literature review, but they do ask for the scale argument that literature reviews presuppose.

Research frontier: mass models beyond the SEMF and student projects

The liquid-drop SEMF of Lecture 4 is still the pedagogical backbone of nuclear binding: volume, surface, Coulomb, asymmetry, and pairing terms explain the broad trends of B/A. Quantitative modern work, however, combines microscopic shell corrections, Bayesian coefficient fits, and machine-learning residuals trained against evaluated mass tables such as AME2020 [27]. Far from stability the smooth SEMF extrapolation fails: shell evolution, continuum coupling, and deformation require microscopic models constrained by rare-isotope data [51]. Community planning documents treat high-precision masses as enabling science for nucleosynthesis pathways and for neutrino-related nuclear matrix elements, because Q values enter both r-process waiting-point estimates and $0\nu\beta\beta$ phase space [52]. What remains uncertain is how far global mass models can be trusted beyond the last

measured point, and how to quote honest uncertainties when several models disagree by mega-electronvolts near the drip lines. Machine-learning approaches can reduce rms residuals, but they must be audited for extrapolation artefacts.

In practice, a modern mass-model paper reports not only an rms residual on known nuclei but also a validation protocol for extrapolation. Students can reproduce a simple leave-one-out test on AME2020 subsets: hide a region of the chart, refit or retrain, and measure the prediction error. That exercise shows why drip-line forecasts need conservative uncertainty bars.

Student directions. (1) Computational fit: fit a_V, a_S, a_C, a_a to a subset of AME2020 even-even masses and quote rms residuals. (2) Data project: identify ten nuclei where $|M_{\text{exp}} - M_{\text{SEMF}}|$ exceeds 5 MeV and correlate them with magic numbers. (3) Critical essay: critique using SEMF coefficients near the drip line for r-process waiting-point estimates.

1.20 Problems with solutions

Problem 4.1 — Binding energy of the α particle

Atomic masses (u): $m(^1\text{H}) = 1.007825$, $m(n) = 1.008665$, $m(^4\text{He}) = 4.002603$. Compute B and B/A for the α particle. Use $c^2 = 931.5\,\text{MeV/u}$.

Solution 4.1

$$\begin{aligned} B &= [2m(^1\text{H}) + 2m(n) - m(^4\text{He})]\,c^2 \\ &= (2 \times 1.007825 + 2 \times 1.008665 - 4.002603)\,\text{u}\,c^2 \\ &= 0.030377 \times 931.5\,\text{MeV} \approx 28.3\,\text{MeV}. \end{aligned}$$

$$B/A \approx 7.07\,\text{MeV}.$$

The α is exceptionally tightly bound for a light nucleus (cluster peak on the B/A curve) [6, 1].

Problem 4.2 — Coulomb coefficient a_C (Petrera 1.1.2)

Using classical electrostatics for a uniformly charged sphere of radius $R = r_0 A^{1/3}$ with $r_0 = 1.2\,\text{fm}$, estimate the SEMF Coulomb coefficient in the term $a_C Z^2/A^{1/3}$. Take $\hbar c \approx 197\,\text{MeV fm}$ and $\alpha \approx 1/137$.

Solution 4.2

$$E_C = \frac{3}{5}\frac{(Ze)^2}{4\pi\varepsilon_0 R} = \frac{3}{5}\frac{\alpha\,\hbar c}{r_0}\frac{Z^2}{A^{1/3}}.$$

$$a_C = \frac{3}{5}\frac{\alpha\,\hbar c}{r_0} \approx \frac{3}{5}\frac{197/137}{1.2} \approx 0.72\,\text{MeV},$$

matching the usual fit [3, 6].

Problem 4.3 — B/A of ^{56}Fe from the SEMF

Use $a_V = 15.5$, $a_S = 16.8$, $a_C = 0.72$, $a_\mathrm{a} = 23\,\mathrm{MeV}$ (pairing neglected). Estimate B/A for ^{56}Fe ($Z = 26$).

Solution 4.3

$$\frac{B}{A} = a_V - \frac{a_S}{A^{1/3}} - a_C\frac{Z(Z-1)}{A^{4/3}} - a_\mathrm{a}\frac{(A-2Z)^2}{A^2}.$$

With $A = 56$, $Z = 26$, $A^{1/3} \approx 3.83$, $A - 2Z = 4$:

$$\begin{aligned} a_V &= 15.5, \\ a_S/A^{1/3} &\approx 4.39, \\ a_C Z(Z-1)/A^{4/3} &\approx 0.72 \times 650/(56 \times 3.83) \approx 2.18, \\ a_\mathrm{a}(A-2Z)^2/A^2 &\approx 23 \times 16/3136 \approx 0.12. \end{aligned}$$

$$B/A \approx 15.5 - 4.39 - 2.18 - 0.12 \approx 8.8\,\mathrm{MeV},$$

near the experimental iron-region maximum [6, 14].

Problem 4.4 — Volume vs surface for light and heavy nuclei

With $a_V = 15.5\,\mathrm{MeV}$ and $a_S = 16.8\,\mathrm{MeV}$, compare the volume and surface contributions to B/A for $A = 16$ and $A = 208$.

Solution 4.4

$B_V/A = a_V = 15.5\,\mathrm{MeV}$ (independent of A); $|B_S|/A = a_S A^{-1/3}$.

A	$a_S A^{-1/3}$ (MeV)	surface/volume
16	$16.8/2.52 \approx 6.7$	$\sim 43\%$
208	$16.8/5.92 \approx 2.8$	$\sim 18\%$

Light nuclei are surface-dominated; heavy nuclei are bulk-dominated [13].

Problem 4.5 — Coulomb energy of ^{208}Pb

Estimate the Coulomb self-energy of ^{208}Pb ($Z = 82$, $R = 1.2\,A^{1/3}\,\mathrm{fm}$) with the uniform-sphere formula. Give E_C in MeV and E_C/A.

Solution 4.5

$$R \approx 1.2 \times 5.92 \approx 7.1\,\text{fm}, \quad E_C = a_C \frac{Z^2}{A^{1/3}} \approx 0.72 \frac{82^2}{5.92} \approx 820\,\text{MeV}, \quad \frac{E_C}{A} \approx 3.9\,\text{MeV}.$$

Coulomb is the main reason B/A falls for heavy nuclei [1, 6].

Problem 4.6 — Asymmetry energy of ^{208}Pb

For ^{208}Pb ($N = 126$, $Z = 82$) with $a_\text{a} = 23\,\text{MeV}$, compute the asymmetry contribution to B and to B/A.

Solution 4.6

$$E_\text{a} = a_\text{a} \frac{(N-Z)^2}{A} = 23 \frac{44^2}{208} = 23 \times 9.31 \approx 214\,\text{MeV}, \quad \frac{E_\text{a}}{A} \approx 1.0\,\text{MeV}.$$

Neutron excess costs hundreds of MeV in total binding, but only about 1 MeV per nucleon at lead [14].

Problem 4.7 — Q value for $d + d \to t + p$ (Petrera 1.3.3)

Binding energies: $B(^2\text{H}) = 2.23\,\text{MeV}$, $B(^3\text{H}) = 8.48\,\text{MeV}$. Compute the Q value of

$$^2\text{H} + {}^2\text{H} \to {}^3\text{H} + p.$$

Also estimate the temperature needed for two deuterons to approach to 1.4 fm against Coulomb repulsion ($k_B = 8.6 \times 10^{-5}\,\text{eV/K}$).

Solution 4.7

Energy release equals the increase in total binding:

$$Q = B_t - 2B_d = 8.48 - 2 \times 2.23 = 4.02\,\text{MeV}.$$

Coulomb barrier at $R = 1.4\,\text{fm}$:

$$E_\text{cm} \simeq \frac{\alpha\,\hbar c}{R} \approx \frac{197/137}{1.4} \approx 1.03\,\text{MeV}.$$

For two equal deuterons in the centre-of-mass frame, each carries half of this kinetic energy. A crude classical thermal threshold follows from $k_B T \sim E_\text{cm}$:

$$T \sim \frac{1.03 \times 10^6\,\text{eV}}{8.6 \times 10^{-5}\,\text{eV/K}} \approx 1.2 \times 10^{10}\,\text{K}.$$

This is a *classical* overestimate: quantum tunnelling through the Coulomb barrier permits fusion at much lower stellar temperatures [3].

Problem 4.8 — Both β modes of ^{64}Cu (Petrera 1.3.5)

Using the SEMF with $a_C = 0.697\,\text{MeV}$, $a_\text{a} = 23.3\,\text{MeV}$, and $M_n - M_p - m_e = 0.782\,\text{MeV}$, show that ^{64}Cu ($A = 64$, $Z = 29$) can β^- decay to ^{64}Zn and β^+ decay to ^{64}Ni. Estimate Q_{β^-} and Q_{β^+} (pairing: even–even final nuclei gain $\delta = \pm 34 A^{-3/4}\,\text{MeV}$ for even–even / odd–odd).

Solution 4.8

$$Q_{\beta^-} = (M_n - M_p - m_e) + [B(64,30) - B(64,29)],$$

$$Q_{\beta^+} = (M_p - M_n - m_e) + [B(64,28) - B(64,29)].$$

$A^{1/3} = 4$ and $\delta_0 = 34/64^{3/4} = 1.503\,\text{MeV}$. Volume and surface cancel. For the $Z = 29 \to 30$ branch,

$$B(64,30) - B(64,29) = -\frac{0.697}{4}(60) - \frac{23.3}{64}(4^2 - 6^2) + 2\delta_0 \approx 0.180\,\text{MeV},$$

whereas for $Z = 29 \to 28$,

$$B(64,28) - B(64,29) = +\frac{0.697}{4}(56) - \frac{23.3}{64}(8^2 - 6^2) + 2\delta_0 \approx 2.569\,\text{MeV}.$$

Atomic-mass bookkeeping gives $(m_n - m(^1\text{H}))c^2 = +0.782\,\text{MeV}$ for β^-, while the free-mass term for β^+ is $(m(^1\text{H}) - m_n)c^2 - 2m_e c^2 = -1.804\,\text{MeV}$. Therefore

$$Q_{\beta^-} \approx 0.782 + 0.180 = 0.962\,\text{MeV} > 0, \quad Q_{\beta^+} \approx -1.804 + 2.569 = 0.765\,\text{MeV} > 0.$$

Both branches are open; maximum $e^\pm$ kinetic energies equal the corresponding Q values up to recoil. The calculation also shows why pairing cannot be omitted: it lowers both even–even daughters relative to the odd–odd parent [3].

Bibliography

[1] R. A. Dunlap, *An Introduction to the Physics of Nuclei and Particles* (2nd ed.), IOP Publishing, Bristol (2023), DOI: 10.1088/978-0-7503-6094-4, Ch. 3 (Nuclear composition and size).

[2] W. Demtröder, *Nuclear and Particle Physics*, Undergraduate Lecture Notes in Physics, Springer, Cham (2023).

[3] S. Petrera, *Problems and Solutions in Nuclear and Particle Physics*, UNITEXT for Physics, Springer, Cham (2019).

[4] F. Terranova, *A Modern Primer in Particle and Nuclear Physics*, Oxford University Press (2021).

[5] S. D'Auria, *Introduction to Nuclear and Particle Physics*, Undergraduate Lecture Notes in Physics, Springer, Cham (2018).

[6] K. S. Krane, *Introductory Nuclear Physics*, Wiley, New York (1988).

[7] R. Hofstadter, "Electron scattering and nuclear structure," Rev. Mod. Phys. **28**, 214 (1956).

[8] H. F. Ehrenberg, R. Hofstadter, U. Meyer-Berkhout, D. G. Ravenhall, and S. E. Sobottka, "High-Energy Electron Scattering and the Charge Distribution of Carbon-12 and Oxygen-16," Phys. Rev. **113**, 666 (1959).

[9] H. Yukawa, "On the interaction of elementary particles. I," Proc. Phys.-Math. Soc. Japan **17**, 48 (1935).

[10] R. D. Woods and D. S. Saxon, "Diffuse surface optical model for nucleon-nuclei scattering," Phys. Rev. **95**, 577 (1954).

[11] H. G. J. Moseley, "The high-frequency spectra of the elements," Phil. Mag. **26**, 1024 (1913); **27**, 703 (1914).

[12] C. F. von Weizsäcker, "Zur Theorie der Kernmassen," Z. Phys. **96**, 431 (1935).

[13] P. Cappellaro, *Introduction to Applied Nuclear Physics* (MIT OpenCourseWare / LibreTexts), CC BY-NC-SA 4.0.

[14] J.-L. Basdevant, J. Rich, and M. Spiro, *Fundamentals in Nuclear Physics: From Nuclear Structure to Cosmology*, Springer, New York (2005).

[15] D. Tong, *Particle Physics*, Lecture notes (University of Cambridge / CERN school notes).

[16] M. G. Mayer, "On closed shells in nuclei. II," Phys. Rev. **75**, 1969 (1949).

[17] O. Haxel, J. H. D. Jensen, and H. E. Suess, "On the "magic numbers" in nuclear structure," Phys. Rev. **75**, 1766 (1949).

[18] T. Schmidt, "Über die magnetischen Momente der Atomkerne," Z. Phys. **106**, 358 (1937).

[19] L. W. Nordheim, "On spins, moments, and shells in nuclei," Phys. Rev. **78**, 294 (1950).

[20] Evaluated Nuclear Structure Data File (ENSDF), National Nuclear Data Center, Brookhaven National Laboratory, `https://www.nndc.bnl.gov/ensdf/`.

[21] NuDat 3, National Nuclear Data Center, Brookhaven National Laboratory, `https://www.nndc.bnl.gov/nudat3/`.

[22] N. J. Stone, "Table of nuclear magnetic dipole and electric quadrupole moments," At. Data Nucl. Data Tables **90**, 75 (2005); updated compilations at NNDC.

[23] W. N. Cottingham and D. A. Greenwood, *An Introduction to Nuclear Physics* (2nd ed.), Cambridge University Press, Cambridge (2001).

[24] H. Geiger and J. M. Nuttall, "The ranges of the α particles from the radioactive substances," Phil. Mag. **22**, 613 (1911).

[25] G. Gamow, "Zur Quantentheorie des Atomkernes," Z. Phys. **51**, 204 (1928).

[26] R. W. Gurney and E. U. Condon, "Wave mechanics and radioactive disintegration," Nature **122**, 439 (1928); Phys. Rev. **33**, 127 (1929).

[27] M. Wang, W. J. Huang, F. G. Kondev, G. Audi, and S. Naimi, "The AME 2020 atomic mass evaluation (II). Tables, graphs and references," Chin. Phys. C **45**, 030003 (2021).

[28] Laboratoire National Henri Becquerel (LNHB), Recommended decay data, `http://www.lnhb.fr/nuclear-data/nuclear-data-table/`.

[29] L. M. Langer, R. D. Moffat, and H. C. Price, Jr., "Low energy beta-ray spectra: P^{32} and Cu^{64}," Phys. Rev. **76**, 1725 (1949).

[30] L. M. Langer and H. C. Price, Jr., "Shapes of the beta-spectra of the forbidden transitions of Sb^{124}, Rb^{86}, Sr^{89}, Y^{91}, and Cs^{137}," Phys. Rev. **75**, 1769 (1949).

[31] D. C. Camp and L. M. Langer, "The shape of the ^{66}Ga positron spectrum and the contribution from $0^+ \to 0^+$ transitions," Phys. Rev. **129**, 1782 (1963).

[32] H. C. Verma, *Nuclear Physics: Fundamentals and Applications*, NPTEL/IIT Kanpur lecture series, `https://hcverma.in/ncl_phy_lectures`.

[33] International Atomic Energy Agency, *LiveChart of Nuclides*, evaluated structure, decay, reaction, and fission-yield data, `https://www-nds.iaea.org/relnsd/vcharthtml/VChartHTML.html`.

[34] T. Kibédi, T. W. Burrows, M. B. Trzhaskovskaya, P. M. Davidson, and C. W. Nestor, Jr., "Evaluation of theoretical conversion coefficients using BrIcc," Nucl. Instrum. Methods Phys. Res. A **589**, 202 (2008), DOI: 10.1016/j.nima.2008.02.051.

[35] D. A. Brown *et al.*, "ENDF/B-VIII.0: The 8th major release of the nuclear reaction data library with CIELO-project cross sections, new standards and thermal scattering data," Nucl. Data Sheets **148**, 1 (2018), DOI: 10.1016/j.nds.2018.02.001.

[36] B. Acharya *et al.*, "Solar fusion III: New data and theory for hydrogen-burning stars," Rev. Mod. Phys. **97**, 035002 (2025), DOI: 10.1103/8lm7-gs18.

[37] S. N. Ghoshal, "An experimental verification of the theory of compound nucleus," Phys. Rev. **80**, 939 (1950), DOI: 10.1103/PhysRev.80.939.

[38] D. Adhikari *et al.* (PREX Collaboration), "Accurate determination of the neutron skin thickness of ^{208}Pb through parity-violation in electron scattering," Phys. Rev. Lett. **126**, 172502 (2021), DOI: 10.1103/PhysRevLett.126.172502.

[39] B. T. Reed, F. J. Fattoyev, C. J. Horowitz, and J. Piekarewicz, "Implications of PREX-II on the equation of state of neutron-rich matter," Phys. Rev. Lett. **126**, 172503 (2021), DOI: 10.1103/PhysRevLett.126.172503.

[40] B. Hu *et al.*, "Ab initio predictions link the neutron skin of ^{208}Pb to nuclear forces," Nature Phys. **18**, 1196 (2022), DOI: 10.1038/s41567-022-01715-8.

[41] E. Epelbaum, H.-W. Hammer, and U.-G. Meißner, "Modern theory of nuclear forces," Rev. Mod. Phys. **81**, 1773 (2009), DOI: 10.1103/RevModPhys.81.1773.

[42] H.-W. Hammer, S. König, and U. van Kolck, "Nuclear effective field theory: Status and perspectives," Rev. Mod. Phys. **92**, 025004 (2020), DOI: 10.1103/RevModPhys.92.025004.

[43] T. Otsuka, A. Gade, O. Sorlin, T. Suzuki, and Y. Utsuno, "Evolution of shell structure in exotic nuclei," Rev. Mod. Phys. **92**, 015002 (2020), DOI: 10.1103/RevModPhys.92.015002.

[44] H. Hergert, S. K. Bogner, T. D. Morris, A. Schwenk, and K. Tsukiyama, "The in-medium similarity renormalization group: A novel ab initio method for nuclei," Phys. Rep. **621**, 165 (2016), DOI: 10.1016/j.physrep.2015.12.007.

[45] J. M. Lattimer and M. Prakash, "The equation of state of hot, dense matter and neutron stars," Phys. Rep. **621**, 127 (2016), DOI: 10.1016/j.physrep.2015.12.005.

[46] J. M. Lattimer, "Neutron stars and the nuclear matter equation of state," Annu. Rev. Nucl. Part. Sci. **71**, 433 (2021), DOI: 10.1146/annurev-nucl-102419-124827.

[47] B. P. Abbott *et al.* (LIGO Scientific Collaboration and Virgo Collaboration), "GW170817: Observation of gravitational waves from a binary neutron star inspiral," Phys. Rev. Lett. **119**, 161101 (2017), DOI: 10.1103/PhysRevLett.119.161101.

[48] M. J. Dolinski, A. W. P. Poon, and W. Rodejohann, "Neutrinoless double-beta decay: Status and prospects," Annu. Rev. Nucl. Part. Sci. **69**, 219 (2019), DOI: 10.1146/annurev-nucl-101918-023407.

[49] M. Agostini, G. Benato, J. A. Detwiler, J. Menéndez, and F. Vissani, "Toward the discovery of matter creation with neutrinoless $\beta\beta$ decay," Rev. Mod. Phys. **95**, 025002 (2023), DOI: 10.1103/RevModPhys.95.025002.

[50] P. Gysbers *et al.*, "Discrepancy between experimental and theoretical β-decay rates resolved from first principles," Nature Phys. **15**, 428 (2019), DOI: 10.1038/s41567-019-0450-7.

[51] H. L. Crawford, K. Fossez, S. König, and A. Spyrou, "A vision for the science of rare isotopes," Annu. Rev. Nucl. Part. Sci. **74**, 141 (2024), DOI: 10.1146/annurev-nucl-121423-091501.

[52] Nuclear Science Advisory Committee, *A New Era of Discovery: The 2023 Long Range Plan for Nuclear Science*, U.S. Department of Energy and National Science Foundation (2023), `https://nuclearsciencefuture.org/`.

[53] S. A. Giuliani, Z. Matheson, W. Nazarewicz, E. Olsen, P.-G. Reinhard, J. Sadhukhan, B. Schuetrumpf, N. Schunck, and P. Schwerdtfeger, "Colloquium: Superheavy elements: Oganesson and beyond," Rev. Mod. Phys. **91**, 011001 (2019), DOI: 10.1103/RevModPhys.91.011001.

[54] N. Schunck and D. Regnier, "Theory of nuclear fission," Prog. Part. Nucl. Phys. **125**, 103963 (2022), DOI: 10.1016/j.ppnp.2022.103963.

[55] I. Counts, J. Hur, D. P. L. Aude Craik, H. Jeon, C. Leung, J. C. Berengut, A. Geddes, A. Kawasaki, W. Jhe, and V. Vuletić, "Evidence for nonlinear isotope shift in Yb^+ search for new boson," Phys. Rev. Lett. **125**, 123002 (2020), DOI: 10.1103/PhysRevLett.125.123002.

[56] I. Angeli and K. P. Marinova, "Table of experimental nuclear ground state charge radii: An update," At. Data Nucl. Data Tables **99**, 69 (2013), DOI: 10.1016/j.adt.2011.12.006.

[57] S. Kraemer *et al.*, "Observation of the radiative decay of the ^{229}Th nuclear clock isomer," Nature **617**, 706 (2023), DOI: 10.1038/s41586-023-05894-z.